Earth-Science Reviews 215 (2021) 103562

Contents lists available at ScienceDirect

Earth-Science Reviews

journal homepage: www.elsevier.com/locate/earscirev

Review article

Interactions of Asian mineral dust with Indian summer monsoon: Recent advances and challenges

Qinjian Jin [a,*], Jiangfeng Wei [b,**], William K.M. Lau [c], Bing Pu [a], Chien Wang [d]

[a] Department of Geography and Atmospheric Science, University of Kansas, Lawrence, KS, USA
[b] Collaborative Innovation Center on Forecast and Evaluation of Meteorological Disasters/Key Laboratory of Meteorological Disaster, Ministry of Education/International Joint Research Laboratory on Climate and Environment Change, Nanjing University of Information Science and Technology, Nanjing, Jiangsu, China
[c] Earth System Science Interdisciplinary Center, University of Maryland, College Park, MD, USA
[d] Laboratoire d'Aerologie, CNRS/UPS, Toulouse, France

ARTICLE INFO

Keywords:
Asian mineral dust
Indian summer monsoon
Interaction

ABSTRACT

The Indian summer monsoon (ISM) is one of the world's strongest monsoon systems that brings about eighty percent of the annual rainfall to the Indian subcontinent and impacts the livelihood of more than a quarter of the world's population. Meanwhile, Asia is the world's second largest dust source—with major deserts in the Middle East, Central and East Asia. The interactions between the Asian dust and the ISM have received increasing attention in recent decades. Dust particles can modulate the circulation and precipitation of the ISM through absorption of solar and terrestrial radiation when suspending in the atmosphere and when deposited in snow and ice at surface and by acting as nuclei of liquid and ice clouds. In turn, the ISM can affect dust emissions, transport, and deposition through atmospheric circulation and wet scavenging. This review provides a) an overview of several physical mechanisms behind the interactions between the ISM rainfall and the Asian dust particularly the Middle East dust, b) a new hypothesis to explain the observed positive correlation between the Middle East dust and the ISM rainfall, and c) a summary of current progress and challenges in dust simulation in climate models. Finally, we propose future research directions aimed at improving dust–monsoon simulations in terms of dust long-term variability, absorbing property, and anthropogenic contributions.

1. Introduction

Monsoon is defined as the seasonal reversal of large-scale wind direction coupled to a strong seasonal cycle of rainfall (e.g., Simpson, 1921; Ramage, 1971; Rao, 1976; Webster, 1987). Most monsoon systems are driven by the seasonal shift in the meridional displacement of the Inter Tropical Convergence Zone (ITCZ), which lags the seasonal north-south migration of subsolar point by 1–2 months (Blandford, 1886; Riehl, 1954; Charney, 1967; Riehl, 1979; Sikka and Gadgil, 1980; Gadgil, 2003; Goswami, 2005; Wang et al., 2014; Gadgil, 2018; Hill, 2019; Geen et al., 2020; (Wang et al., 2021). Monsoon strength is significantly modulated by land–ocean thermal contrast (Halley, 1753; Webster, 1987; Gadgil, 2003; Wu et al., 2012; Roxy et al., 2015; Jin and Wang, 2017; Gadgil, 2018) and interhemispheric temperature

Abbreviations: AOD, Aerosol Optical Depth; ASM, Asian Summer Monsoon; CALIOP, Cloud-Aerosol Lidar with Orthogonal Polarization; CALIPSO, Cloud-Aerosol Lidar and Infrared Pathfinder Satellite Observation; CAM5, Community Atmosphere Model version 5; CCN, Cloud Condensation Nuclei; CESM, Community Earth System Model; DOD, Dust Optical Depth; EASM, East Asian Summer Monsoon; EHP, Elevated Heat Pump; EMIT, The Earth Surface Mineral Dust Source Investigation; GEOS-5, Goddard Earth System Model Version 5; GPCP, Global Precipitation Climatology Project; GPM, Global Precipitation Measurement; IN, Ice Nuclei; ISM, Indian Summer Monsoon; ITCZ, Inter Tropical Convergence Zone; ITD, Inter Tropical Discontinuity; MERRA-2, Modern Era Retrospective-Analysis for Research and Applications, version 2; MISR, Multi-angle Imaging SpectroRadiometer; MODIS, MODerate resolution Imaging Spectroradiometer; MPAS, Model of Prediction Across Scales; MV-EOF, Multi-Variate Empirical Orthogonal Function; PNWI, Pakistan/Northwest India; RegCM4, Regional Climate Model version 4; SDE, Snow-Darkening Effect; UTC, Coordinated Universal Time; WRF-Chem, Weather Research and Forecasting model coupled with online Chemistry.

* Corresponding author at: Department of Geography and Atmospheric Science, University of Kansas, 1475 Jayhawk Boulevard, Lawrence, KS 66045, USA.
** Corresponding author at: Collaborative Innovation Center on Forecast and Evaluation of Meteorological Disasters/Key Laboratory of Meteorological Disaster, Ministry of Education/International Joint Research Laboratory on Climate and Environment Change, Nanjing University of Information Science and Technology, Nanjing, Jiangsu, China 210044
E-mail addresses: jqj@ku.edu (Q. Jin), jwei@nuist.edu.cn (J. Wei).

https://doi.org/10.1016/j.earscirev.2021.103562
Received 29 August 2020; Received in revised form 2 January 2021; Accepted 15 February 2021
Available online 21 February 2021
0012-8252/© 2021 The Author(s). Published by Elsevier B.V. This is an open access article under the CC BY-NC-ND license (http://creativecommons.org/licenses/by-nc-nd/4.0/).

differences (Wang et al., 2011; Chiang and Friedman, 2012; Friedman et al., 2013). Summer monsoon usually brings warm and humid air from tropical oceans to continents and thus causes heavy rainfall. By contrast, winter monsoon brings cold and dry air from continents to oceans (e.g., Chang et al., 2006; Dimri et al., 2016). More research efforts have been devoted to summer monsoon than winter monsoon since the former plays more important roles in moisture transport, cloud formation, and the hydrological cycle.

The Indian summer monsoon (ISM), also known as the South Asian summer monsoon, is one of the world's strongest monsoon systems (Wang and LinHo, 2002; Wang et al., 2014; Wang et al., 2017). At the end of May and in early June, the meridional shift of the subsolar point drives the northward propagation of the ITCZ, which brings abundant moist air from the Southern Hemisphere to the Northern Hemisphere causing strong convection over the Northern Indian Ocean. As the subsolar point and ITCZ propagate further north in mid-June, the Indian subcontinent warms up by absorption of the increasing solar radiation at a greater rate than the Indian Ocean does, forming a strong ocean–land thermal gradient, which drives strong low-level southwesterly winds that transport water vapor from the tropical Indian Ocean and the Arabian Sea towards the Indian subcontinent (Gadgil, 2003, 2018; Hari et al., 2020). The sensible heat flux from the Earth's surface to the atmosphere over the vast Eurasian Continent, especially over the Tibetan Plateau and the Iranian Plateau, further strengthen the ISM circulation by increasing the south–north temperature gradient in the mid-troposphere in July (Wu et al., 2012; Wu et al., 2017). This sensible heat together with the strong latent heat released from intense monsoon convection drives the ISM to reach its peak in July and August (Singh et al., 2007; Rajeevan et al., 2010; Ratnam et al., 2014). As the ITCZ moves southward in August, the ISM demises in September.

Besides the dominant roles of the ITCZ and ocean–land thermal contrast playing in the ISM system, aerosols from both natural and anthropogenic emissions can further modulate the ISM system. The heavy aerosol layers (mainly anthropogenic aerosols, including black carbon and sulfate) over South Asia can cool the surface by scattering and absorbing solar radiation, which reduces the ocean–land thermal contrast and in turn weakens the ISM (Ramanathan et al., 2005; Meehl et al., 2008; Kumari and Goswami, 2010; Bollasina et al., 2011), the so-called "solar dimming" or "global dimming" effect (Stanhill and Cohen, 2001). On the other hand, absorbing aerosols (e.g., black carbon and mineral dust) that accumulate over the southern slope of the Tibetan Plateau can heat the mid-troposphere, pumping the air from South to North India and strengthening monsoon convection over North India (Lau et al., 2006). This is referred to as the "elevated heat pump (EHP)" effect (Lau and Kim, 2006; Lau et al., 2009; Lau and Kim, 2011; Lau, 2016; Lau et al., 2016; Lau and Kim, 2017). Moreover, absorbing aerosols can also modulate the meridional gradient of sub-cloud moist static energy (MSE) over the Indian subcontinent and shift the monsoonal deep convection northwestward (Wang et al., 2009b). When deposited on snow and ice on the Tibetan Plateau, these absorbing aerosols change land surface albedo and energy budget, modifying the circulation and precipitation over both the ISM and East Asian monsoon regions (Lau and Kim, 2018; Rahimi et al., 2019). These different and competing effects of aerosols on the ISM have confounded aerosol–monsoon interactions (Lee et al., 2013; Lee and Wang, 2015) and spurred debates about whether aerosols strengthen or weaken the ISM system (Meehl et al., 2008; Dave et al., 2017).

Recently, studies found that remote dust aerosols from the Middle East can also strongly modulate the variability of ISM system (e.g., Jin et al., 2014; Vinoj et al., 2014). Fig. 1 shows the summertime aerosol

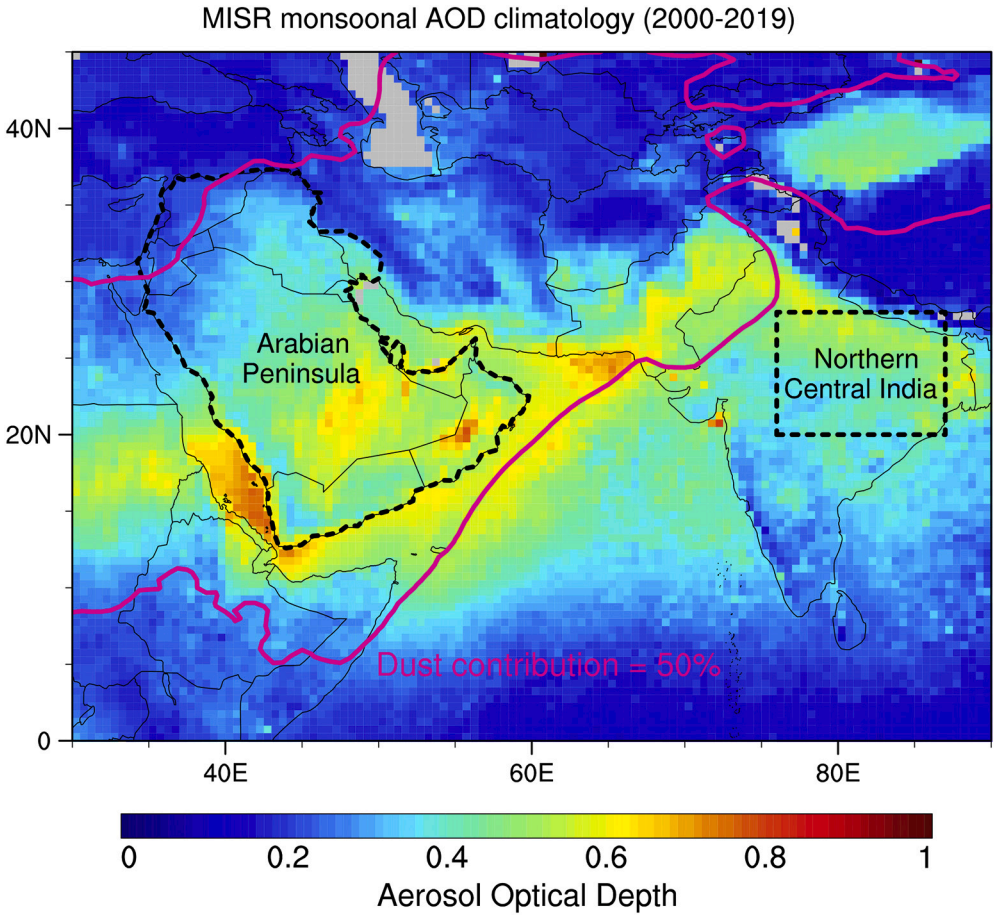


Fig. 1. Domain of interest. Two subregions are highlighted for further analysis: the Arabian Peninsula and Northern Central India (20°–28° N, 76°–87° E). The shadings are monsoonal (June–July–August–September) aerosol optical depth (AOD) from MISR averaged over the period of 2000–2019. Missing values are denoted in grey shading. The red contour indicates regions where dust contributes ≥ 50% to the total AOD based on MERRA-2 reanalysis. MERRA-2 = Modern Era Retrospective-Analysis for Research and Applications, version 2; MISR = Multi-angle Imaging SpectroRadiometer. (For interpretation of the references to color in this figure legend, the reader is referred to the web version of this article.)

optical depth (AOD) climatology in this region. Over the Arabian Peninsula and the northwestern Arabian Sea, more than 50% of the AOD is contributed by mineral dust (Jin et al., 2018). Tons of dust aerosols emitted from the Arabian Peninsula and its surrounding areas are transported to the Arabian Sea by the strong northwesterly "Shamal" winds during boreal summer (Jin et al., 2018). These dust aerosols over the Arabian Sea could heat the lower and mid-troposphere, forming a heat low over the Arabian Sea. This heat low strengthens the southwestern monsoon branch, which favors the moisture transport from the Arabian Sea to the Indian subcontinent and in turn increases rainfall in most parts of the Indian subcontinent (Jin et al., 2014; Vinoj et al., 2014; Jin et al., 2015; Solmon et al., 2015; Jin et al., 2016a).

Although most studies agree that the Middle East dust aerosols can strengthen the ISM system by heating the troposphere, they demonstrate large discrepancies in the ISM rainfall responses in terms of spatial pattern and magnitude. Observations showed that AOD over the Arabian Sea and the southern Arabian Peninsula is significantly and positively correlated with the ISM rainfall in the southwest coastal regions, Northern Central India, and the southern slope of the Tibetan Plateau (Jin et al., 2014; Jin et al., 2015). A global model simulation showed that the monsoonal rainfall responses to dust are negative in Northeast India yet positive in South India (Vinoj et al., 2014). One high-resolution regional model simulation well captured the observed ISM rainfall response patterns to dust (Jin et al., 2015), while another regional model study showed a completely different pattern of rainfall response (Solmon et al., 2015). We will discuss the potential causes of the inconsistent monsoon rainfall responses to Arabian dust aerosols and uncertainties in modeling studies.

More recently, the influence of the ISM on dust emissions and transport in the Middle East and the Arabian Sea is also addressed (Sharma and Miller, 2017; Attada et al., 2018). The observed positive correlation between ISM rainfall and dust is attributed to the effect of the prevailing monsoon circulation on dust emissions over the Arabian Peninsula and transport to the Arabian Sea (Sharma and Miller, 2017). Strong monsoons are found to strengthen the circulation and thermodynamic processes over the Arabian Peninsula through Rossby wave (Rodwell and Hoskins, 2001; Attada et al., 2018). However, to what extent could the monsoon circulations affect the dust emissions over the Arabian Peninsula is still an open question and will be discussed in this review.

It is worth noting that almost all of the current studies have focused on the monsoon–dust interactions within the seasonal timescale partially due to a lack of long-term observations of dust aerosols in a large region that covers South Asia and the Middle East (Fig. 1) as well as challenges in simulating dust interannual and interdecadal variability by most global climate models (Evan et al., 2014; Evan, 2018; Pu and Ginoux, 2018). We will examine dust–monsoon interactions on the interdecadal timescale (1979–2019) using proxy data of dust variations and observed ISM rainfall.

In this paper, we first review recent studies on the interactions between the ISM system and aerosols from both local and remote sources on seasonal timescale in Sections 2–3, with a focus on the dust aerosols from the Middle East. Several hypotheses proposed to explain the monsoon–dust interactions are summarized. The influences of the ISM on dust emissions and transport are discussed in Section 4. Two additional hypotheses that focus on dust–monsoon interaction on the interdecadal timescale and the extended impacts of the Middle East dust on the whole Asian summer monsoon are presented in Section 5. Current challenges and solutions in simulating dust long-term variability, absorbing property, anthropogenic contributions, and the associated climatic impacts are proposed in Section 6, followed by a summary of the review in Section 7. It should be pointed out that this paper is not intended to be a comprehensive review of the ISM system, but rather a specific review of dust–monsoon interaction, which is an important component of the ISM system and have been advanced by recent studies.

2. Impacts of local dust aerosols on the ISM system

The impacts of dust aerosols on the ISM system have been studied for decades, mainly on local dust and anthropogenic aerosols over the Indian subcontinent and the Tibetan Plateau in early studies (Sanap and Pandithurai, 2015 and references therein). Although the dust aerosols over the Himalayas and Tibetan Plateau have four sources—East Asia (the Taklamakan and Gobi Deserts), the Thar Desert at the India–Pakistan border, the Middle East, and North Africa (Hu et al., 2020), here we consider them as local dust because these dust and black carbon aerosols are located over the Indian subcontinent and the Himalayas when they work as a heating source in the troposphere to influence the ISM system. The following sections review several physical mechanisms behind local dust–monsoon interactions.

2.1. "Elevated Heat Pump" effect

Dust aerosols over the Tibetan Plateau have been shown to be able to influence the Asian monsoon at the seasonal timescale (e.g., Lau et al., 2006). The monsoon onset is mainly driven by the strong ocean–land thermal gradient while monsoon maximum around July is sustained by latent heating in the mid- and upper-troposphere due to heavy precipitation. The dust induced EHP could enhance the ocean–land thermal gradient during pre-monsoon and monsoon onset and further amplify the mid- and upper-troposphere warming during monsoon maximum by enhancing monsoonal precipitation and thus latent heating.

During early months of the pre-monsoon season from March to April, dust aerosols can be transported to the north slopes of the Tibetan Plateau from the deserts in western China and to the south slopes from the deserts in the Middle East and Pakistan. The dust aerosols, together with black carbon in the south slopes of the plateau, heat up the air by absorption of solar radiation, resulting in a warm anomaly in the mid-to-upper troposphere over the plateau and consequently enhancing the ocean–land thermal gradient. Later in May and early June, radiation-dynamical feedback processes are induced. As the warmer air rises over the plateau, it enhances the upper-tropospheric meridional temperature gradient, increase the transport of Middle East dust to the Indian subcontinent, and draws in additional moisture from southern Arabia Sea and the Indian Ocean. The feedback results in an earlier onset of the ISM. The feedback continues to intensify the ISM rainfall during the monsoon maximum in July, resulting in more latent heating and a much warmer troposphere. In late July through August, the feedback is weakened due to increased washout of dust and black carbon by heavy monsoon precipitation. Fig. 2 schematically shows stronger monsoon circulations and enhanced clouds and monsoonal rainfall over the Indian subcontinent in a "dirty" compared to a "clean" monsoon (i.e., relatively high and low concentrations of dust and black carbon aerosols over South Asia, respectively) due to the absorbing aerosols-induced warming over the Tibetan Plateau. The above feedback processes are collectively referred to as the "Elevated Heat Pump (EHP)" effect of absorbing aerosols on the ISM, with dust aerosols playing a major role (Lau and Kim, 2006; Lau et al., 2006; Lau et al., 2008; Lau et al., 2009; Lau and Kim, 2010). The EHP hypothesis is proposed mainly through model simulations and has been subject to debate (Nigam and Bollasina, 2010; Lau and Kim, 2011; Nigam and Bollasina, 2011), based on different interpretation of observations (Kuhlmann and Quaas, 2010; Wonsick et al., 2014). Recently, more modeling studies that support the EHP mechanism affecting multi-scale variability of the Asian summer monsoon have emerged (D'Errico et al., 2015; Gu et al., 2015; Lau et al., 2016; Lau and Kim, 2017). EHP effects by absorbing aerosols over other regions, such as Northwest China (Tang et al., 2018) and the Arabian Sea (Vinoj et al., 2014; Jin et al., 2015) have been identified. Possible dust impact on the response of the Asian summer monsoon to El Niño have also been reported (Kim et al., 2016; Lau, 2016; Li et al., 2016).

It is important to note that EHP involves not only local aerosol sources over the Indian subcontinent, but also the transported dust from

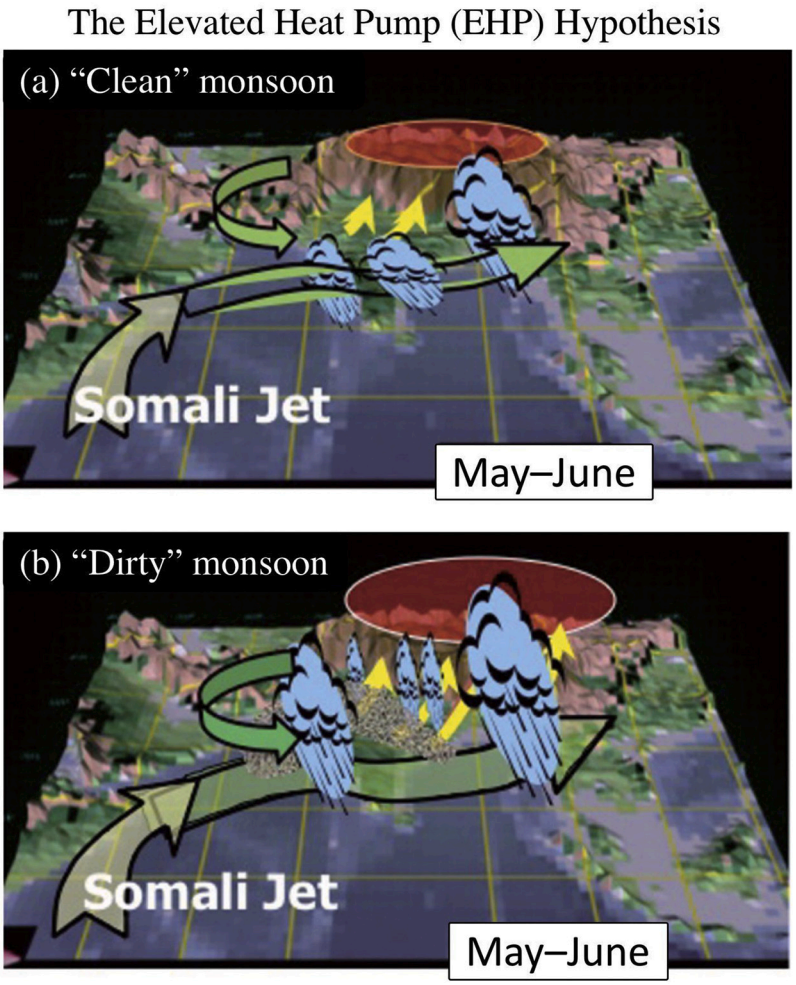


Fig. 2. A schematic comparing different monsoonal circulations and rainfall under "clean" and "dirty" scenarios, i.e., relatively low and high concentrations of dust and black carbon aerosols, respectively over India and the Tibetan Plateau. The absorbing aerosols can strengthen the southwest monsoonal circulations and thus increase clouds and rainfall over the Indian subcontinent (modified from Lau et al. (2016)).

remote deserts in the Middle East (Hu et al., 2020). EHP-induced increase in low-level southwesterlies over the Arabian Sea can transport more dust from the Middle East deserts and moisture from the Arabian Sea onto the Indian subcontinent, fueling the monsoonal precipitation, and replenishing dust lost due to washout by increased precipitation, sustaining the EHP induced dynamics effects through the entire monsoon season (Lau et al., 2020). It is also worth noting that it is the cross-equatorial monsoon circulations over the northern Indian Ocean that transport most of the water vapor required to feed the heavy monsoon precipitation, in comparison to the contributions of water vapor flux over the Arabian Sea and Bay of Bengal (e.g., Xavier et al., 2007; De et al., 2015; Hazra et al., 2015). Therefore, the impact on ISM rainfall by enhanced moisture transport over the Arabian Sea induced by absorbing aerosols through the EHP effect needs to be further examined in a broader context of possible interactions with the aforementioned moisture sources.

2.2. *Moist static energy in sub-cloud layer*

Absorbing aerosols can also modulate the ISM rainfall through perturbing the moist static energy in sub-cloud layer (Wang et al., 2009b). Black carbon aerosols capped in the planetary boundary layer dominate the absorbing aerosols over India. By absorbing solar radiation, black carbon can heat up the planetary boundary layer and thus increases the moist static energy in the sub-cloud layer. Consequently, the black carbon-induced perturbation in moist static energy drives a northward shift of both the ISM rainfall belt (Wang et al., 2009b) and the Intertropical Convergence Zone (ITCZ) (Kovilakam and Mahajan, 2016). Although this hypothesis is based on black carbon, local absorbing dust aerosols can also influence the monsoon in a similar way given that dust aerosols are the second largest contributor to aerosol absorbing optical depth over India (Wang et al., 2009a). But such an influence would be weaker than that from black carbon due to much weaker absorption efficiency on solar radiation by dust. In the future, the impacts of local dust aerosols on the moist static energy in sub-cloud layer needs to be addressed and compared with the impacts of black carbon.

2.3. *Snow-darkening effect (SDE)*

SDE refers to the increased absorption of solar radiation by the land surface due to reduction of surface albedo by deposition of light absorbing aerosols (dust, soot and organic carbon) on snow covered surface (Warren and Wiscombe, 1980; Flanner et al., 2009; Sarangi et al., 2020; Wang et al., 2020). When occurred persistently over large areas, SDE can result in changes in surface energy balance affecting diabatic heating and circulation of the overlying atmosphere (Lau et al., 2010; Gautam et al., 2013; Qian et al., 2014; Yasunari et al., 2015). Although the SDE could cause significant climatic impacts in the Indian subcontinent, the dynamical and hydrological responses to the SDE have not been examined due to lacks of (1) a representation of black carbon

and dust in snow in climate models with on-line chemistry and (2) frequent (e.g., daily) snow impurity measurements at different locations that are necessary for model validation and evaluation (Qian et al., 2014). Until recently, based on numerical experiments with the NASA Goddard Earth Observing System, Version 5 (GEOS-5) model, Lau and Kim et al. (2018) showed that SDE on snow cover of the Himalayas and southern Tibetan Plateau in May–June can trigger a sequence of feedback processes, starting with increased net surface solar radiation, rapid snowmelt, warming of the Tibetan Plateau surface and upper troposphere. These are followed by strengthened low-level southwesterly and enhanced Middle East dust transport across the Arabian Sea to the Himalayas foothills and northern India. The warming is amplified and sustained through June–July–August, by increased latent heating from enhanced precipitation in northern India, due to the EHP effect. The enhanced heating spurs an anomalous upper level Rossby wave train spanning Eurasia, South Asia and East Asia, in conjunction with an enhanced Tibetan Anticyclone, a weakening of the subtropical westerly jet stream, and a northward displacement of the *Mei-Yu* rain band over East Asia (Fig. 3).

Using the Community Earth System Model (CESM), Rahimi et al. (2019) found similar results, indicating strong SDE due to black carbon and dust facilitates rapid snowmelt and surface warming of the TP in the early monsoon season. The warming amplified and extended to the upper troposphere via EHP feedback can induce stronger low-level westerlies during the peak monsoon seasons over the Arabian Sea, furnishing the Indian subcontinent with enhanced moisture and precipitation during peak monsoon season. Shi et al. (2019) emphasized the importance of the SDE-induced surface heat low over Central Asia and Western TP in enhancing advection of drier continent air over northern India in May–June. Das et al. (2020) invested the relative response of the ISM to the SDE and direct radiative effect of dust aerosols and found that the SDE tends to reduce monsoonal rainfall in pre-monsoon season while the DRE of dust facilitates more moisture transport towards the northern India through the EHP mechanism, resulting in enhanced rainfall during monsoon season. In summary, the SDE seems to weaken the ISM system, opposing the EHP effect.

3. Impacts of remote dust aerosols on the ISM system

Besides dust aerosols over the Indian subcontinent, remote dust aerosols over the Middle East and the Arabian Sea can exert significant impact on the ISM system due to their higher concentrations and strong transport by monsoon low level southwesterlies (Fig. 4).

3.1. Dust emission in the Middle East

The Middle East is the world's second largest mineral dust source region following North Africa. Fig. 4 shows the spatial patterns of the climatology (June 2000–May 2020) of seasonal AOD and dust optical depth (DOD) from multiple datasets. Three datasets demonstrate consistent seasonal variations of AOD: high AOD (0.5–0.8) cover most parts of the Arabian Peninsula in pre-monsoon (March–April–May); AOD further increase and reach peak values (0.8–1.0) in monsoon (June–July–August–September) over a large area of the domain, especially over the Arabian Sea; AOD decrease in post-monsoon (October–November–December) and reach a minimum in winter (January–February). DOD manifests similar seasonal variations to AOD. In monsoon when DOD hits the peak, about 50%–90% of the total AOD is attributable to DOD in the Middle East, 38%–54% over the Arabian Sea, 50%–85% in Pakistan and Northwest India (i.e., the local dust source region), depending on various satellite and reanalysis datasets (Jin et al., 2018). Note that both AOD and DOD over the Middle East and the Arabian Sea reach their maxima in the monsoon season.

The spatiotemporal variations in dust aerosols over this region are largely determined by circulations at various spatial scales, because land surface properties (e.g., soil moisture) of the dust sources in the Arabian Peninsula have relatively small seasonal variations. Based on the prevailing weather conditions that generate dust emissions, dust storms can generally be classified into four typical categories generated by: 1) cold-front, 2) meso- and sub-meso scale complexes, 3) tropical disturbances,

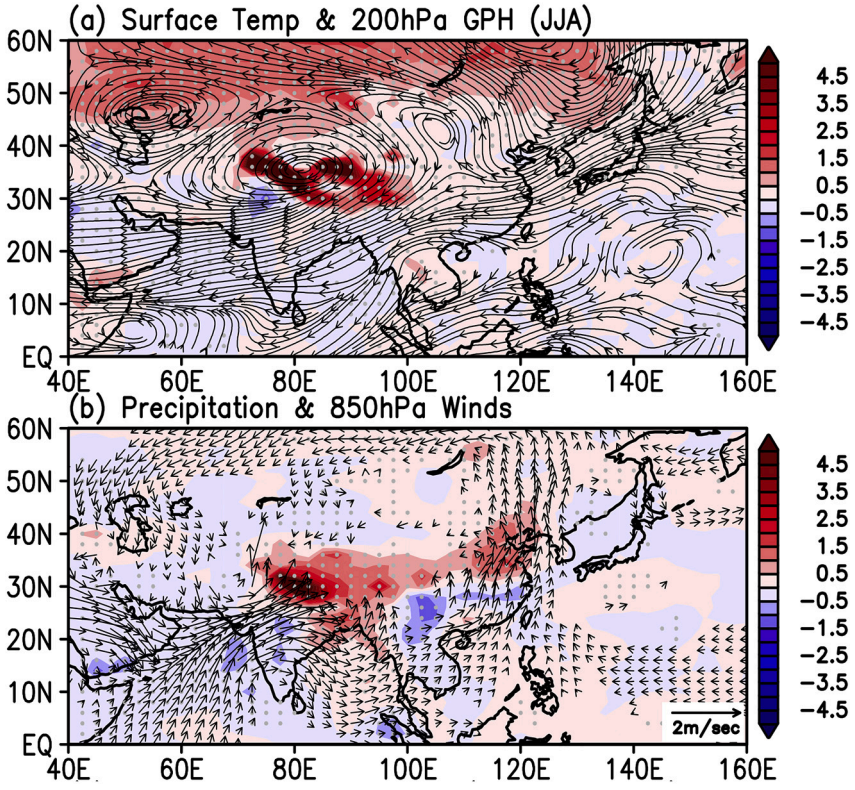


Fig. 3. Spatial patterns of simulated changes for June–July–August by GEOS-5 model due to the snow-darkening effect of dust, black carbon, and organic carbon aerosols over the Tibetan Plateau and the Himalaya foothills in (a) surface temperature (°C) and streamlines at 200 hPa, and (b) precipitation (mm day^{-1}) and 850 hPa winds (m s^{-1}). The simulations are for the period of 2002–2011. The differences are calculated between two sets of simulations with and without aerosols' impact on the snow's surface albedo. Grey dots represent grid cells where changes are statistically significant at 95% confidence level. GEOS-5= Goddard Earth Observing System, Version 5 (adapted from Lau and Kim, 2018).

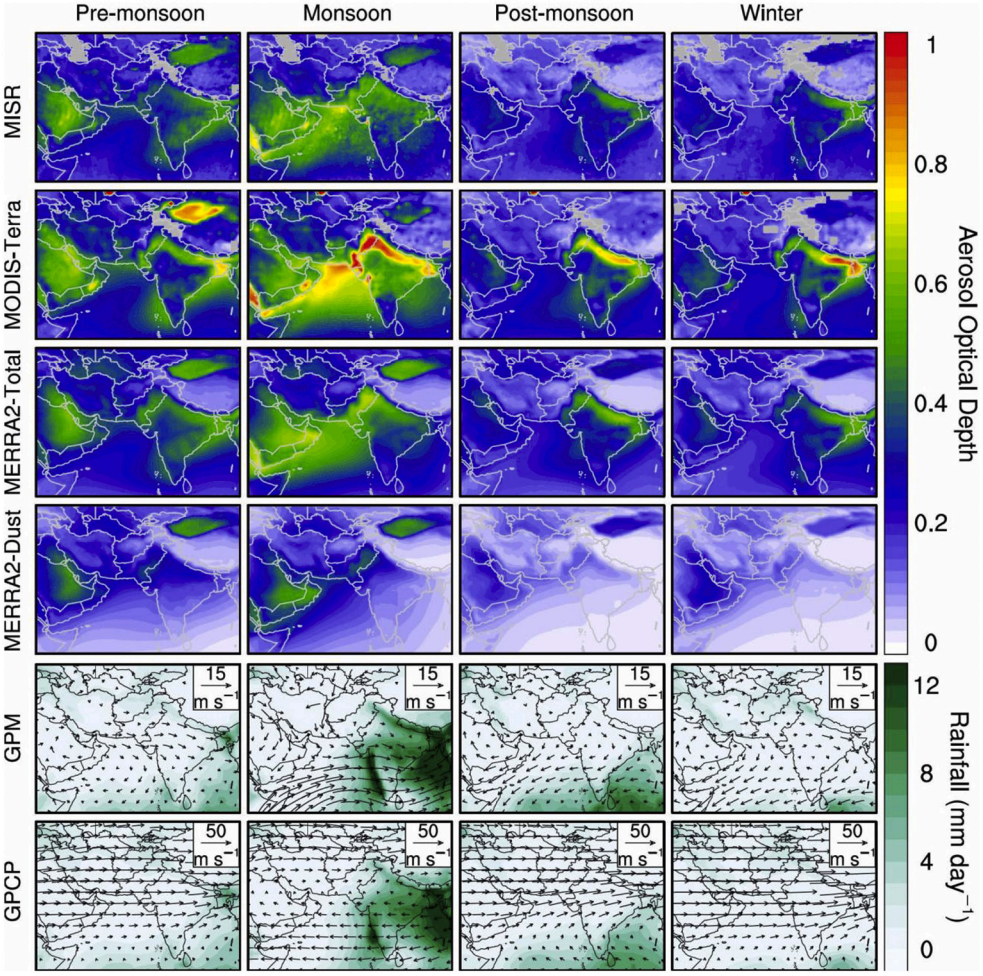


Fig. 4. Spatial patterns of climatological (June 2000–May 2020) AOD, rainfall rate (mm day^{-1}) and winds (m s^{-1}) at 850 and 200 hPa in four seasons. AOD data are from MISR, MODIS-Terra, and MERRA2; rainfall data are from GPM and GPCP; wind data are from MERRA2. The grey shading in the first two rows represents missing values. Pre-monsoon, monsoon, post-monsoon, and winter seasons cover March–April–May, June–July–August–September, October–November–December, and January–February, respectively.

and 4) cyclogenesis (Lei and Wang, 2014). Fig. 5 shows examples of three of the four dust storm types: a cold frontal system caused a dust storm in the southern Arabian Peninsula that was transported southward to the northern Arabian Sea on February 2, 2008 (e.g., Cuevas Agulló, 2013); a meso-scale haboob generated a very strong dust storm in the similar area on July 29, 2018 (e.g., Anisimov et al., 2018); a cyclogenesis triggered a dust storm in Iraq on August 31, 2015 and was transported to the Persian Gulf during the next two days (e.g., Francis et al., 2019). Tropical disturbances occur only infrequently in this region. Statistical analysis of dust storms in the western United States from 2003 to 2013 shows that dust storms triggered by tropical disturbances and cyclogenesis have the longest lifetime (4–21 h) and meso- to sub-meso scale dust storms have shorter durations (2–5 h), but with the highest frequency of occurrence, and rate of dust emissions (Lei and Wang, 2014), which are supported by Fig. 4. It is these different types of dust storms that together result in extremely high dust loadings in summer over the Middle East. However, the spatiotemporal characteristics of these dust storms, and how they have evolved during the past two decades remain largely unknown and unexplored.

3.2. Dust transport to the Arabian Sea

Abundant quantities of dust aerosols are transported to the Arabian Sea from the surrounding land mass in summer. So far, four dust source regions and four corresponding transport pathways have been identified. The four source regions are the Arabian Peninsula (Ramaswamy et al., 2017; Jin et al., 2018; Kumar et al., 2020), Horn of Africa (Léon and Legrand, 2003), deserts in Iran and Afghanistan (e.g., the Karakum desert and Sistan Basin; Kaskaoutis et al., 2016; Kaskaoutis et al., 2018; Rashki et al., 2019), and the Thar Desert at the Pakistan and Indian border (Tindale and Pease, 1999; Badarinath et al., 2010). Fig. 6 shows the back-trajectories of air mass during 100 dusty days over the Arabian

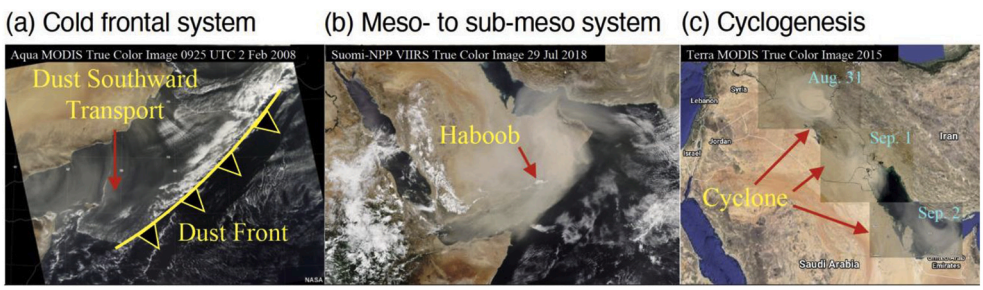


Fig. 5. Three typical dust storm types over the Middle East and the Arabian Sea: true color satellite images and the corresponding weather conditions. (a) Dust storm generated by a cold front on February 2, 2008 over the southern Arabian Peninsula and transported to the northern Arabian Sea. (b) Dust storm caused by a meso-scale haboob on July 29, 2018 over the southern Arabian Peninsula. (c) Dust storm triggered by cyclogenesis on August 31, 2015 over Iraq and transported to the Persian on September 1 and 2.

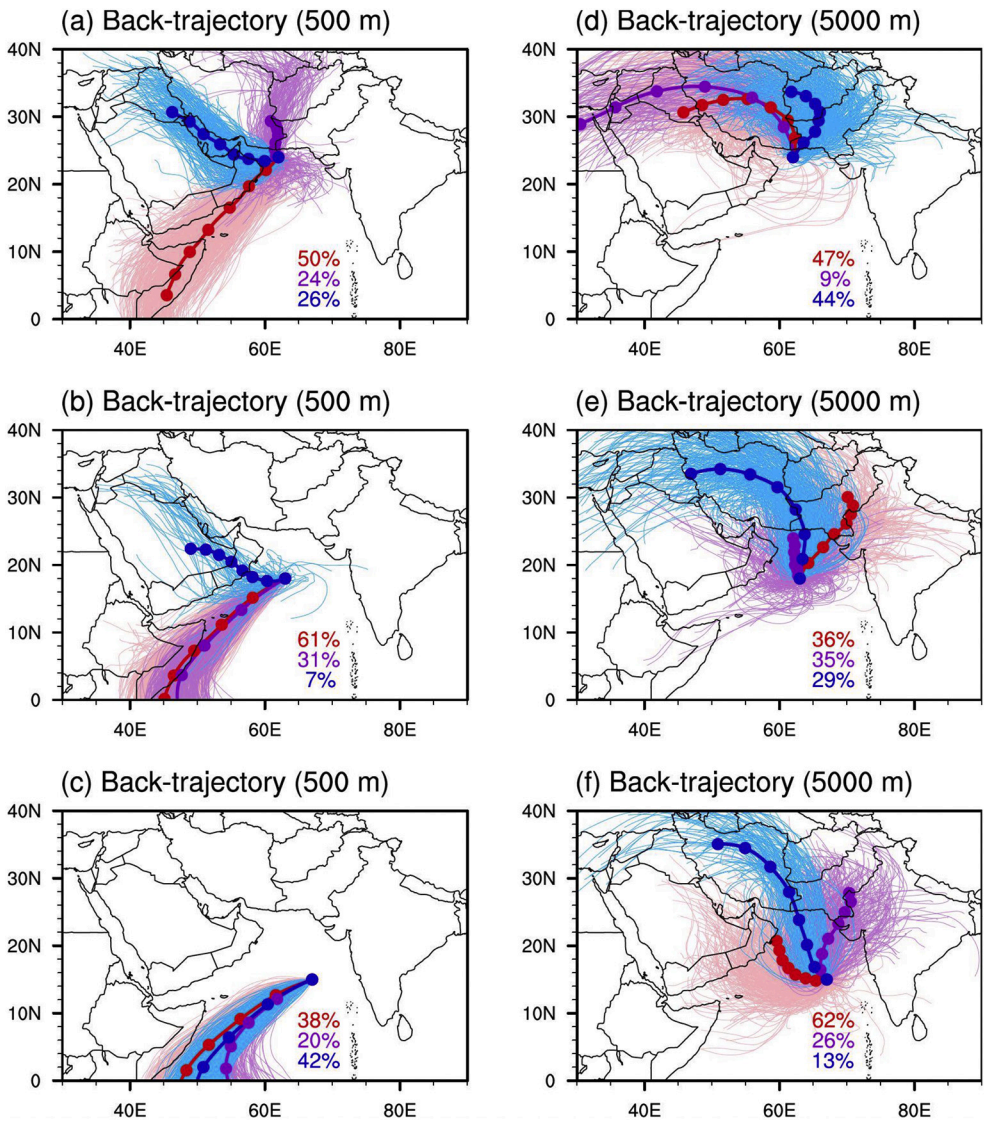


Fig. 6. Back-trajectory analysis of dust transport pathways from dust source regions to the Arabian Sea. Three locations from northwest to southeast of the Arabian Sea were selected, over which the back trajectories of air masses were performed. The left and right columns represent back trajectories at the altitude of 500 and 5,000 m, respectively. Various colors of curves indicate various clusters of these back trajectories represented by thick lines with solid cycles overlaid. Each cycle represents the location of air mass that is 12 h ahead or behind its neighbors, so totally it tracks back to 84 h. The numbers represent the percent of back trajectories in each cluster in the total back trajectories. Totally 100 dusty days (10 in each summer) were selected in June–July–August from 2003 to 2012 for the back-trajectory analysis based on area-averaged MODIS-Aqua daily AOD over the Arabian Sea (8°–25° N, 45°–75° E). 27 ensemble simulations were produced at each location on each dusty day by slightly offsetting the meteorological data by ±1 meteorological grid points in horizontal directions and by ±0.01sigma unit (~250 m) in the vertical direction (copied from Jin et al. (2018)). (For interpretation of the references to color in this figure legend, the reader is referred to the web version of this article.)

Sea selected in summer from 2003 to 2012. The dust aerosols over the northern Arabian Sea have four transport pathways: along the Iraq–Persian Gulf–Gulf of Oman by the northwest "Shamal" wind, along the Iran–Afghanistan border by the north "Levar" wind, and along the coastal line of Somali by the southwest monsoon flow at 500 m altitude and along the northern branch of the monsoonal anti-cyclone at 5000 m altitude. Fig. 7 demonstrates a summertime dust storm extending from surface up to 6 km altitude over the Arabian Peninsula, the Arabian Sea, and Iran–Afghanistan and residing in the troposphere for at least 1 day, which implies that the dust transport from the surrounding source regions to the Arabian Sea in the mid to upper troposphere is possible. Based on Fig. 7, it is worth noting that (1) the aerosol layer is slightly higher over ocean than over land; (2) daytime observations of CALIOP suffers larger noise than those in nighttime; and (3) mixing of dust with other aerosol species seems to be more frequent in daytime than in nighttime, although possible contamination of aerosol mixing states due to the larger daytime noise cannot be ruled out. Over the central Arabian Sea, dust aerosols are transported from the Arabian Peninsula and the Horn of Africa at lower troposphere and share the similar transport pathways to that over the northern Arabian Sea in the mid and upper troposphere. Over the southern Arabian Sea, dust aerosols in the lower troposphere are transported mostly from the Horn of Africa. In the mid-to-upper troposphere, they are transported from all the surrounding land masses, except the Horn of Africa.

The transported dust aerosols over the Arabian Sea are readily accumulated along the so-called "Inter-Tropical Discontinuity (ITD)" area that is defined as areas with near-zero meridional wind (Rashki et al., 2019), as shown in Fig. 8. The northwesterly "Shamal" wind from the Arabian Peninsula and the northerly "Levar" wind from the border of Iran and Afghanistan are confluent with the southwesterly monsoon wind over the central and north Arabian Sea in the lower troposphere. The confluent flow extends dust aerosols to higher altitudes up to 5–6 km (Fig. 7), which favors the accumulation of dust aerosols and consequently results in higher dust concentrations in the atmospheric column over the Arabian Sea along the ITD areas, as seen in Fig. 8.

3.3. *Impacts of dust–radiation interaction on the ISM*

3.3.1. *Observed dust–monsoon relationship*

High aerosols loadings over the southern Arabian Peninsula and the Arabian Sea are positively correlated with the ISM rainfall on various timescales. To the best of our knowledge, Rahul et al. (2008) was the first study that tried to link the variations in ISM rainfall to AOD anomalies over the Arabian Sea. They found that two drought years of 2002 and 2004 with monsoonal rainfall reduction in 50% and 15% of the long-term climatology (1998–2007) in July, respectively, were

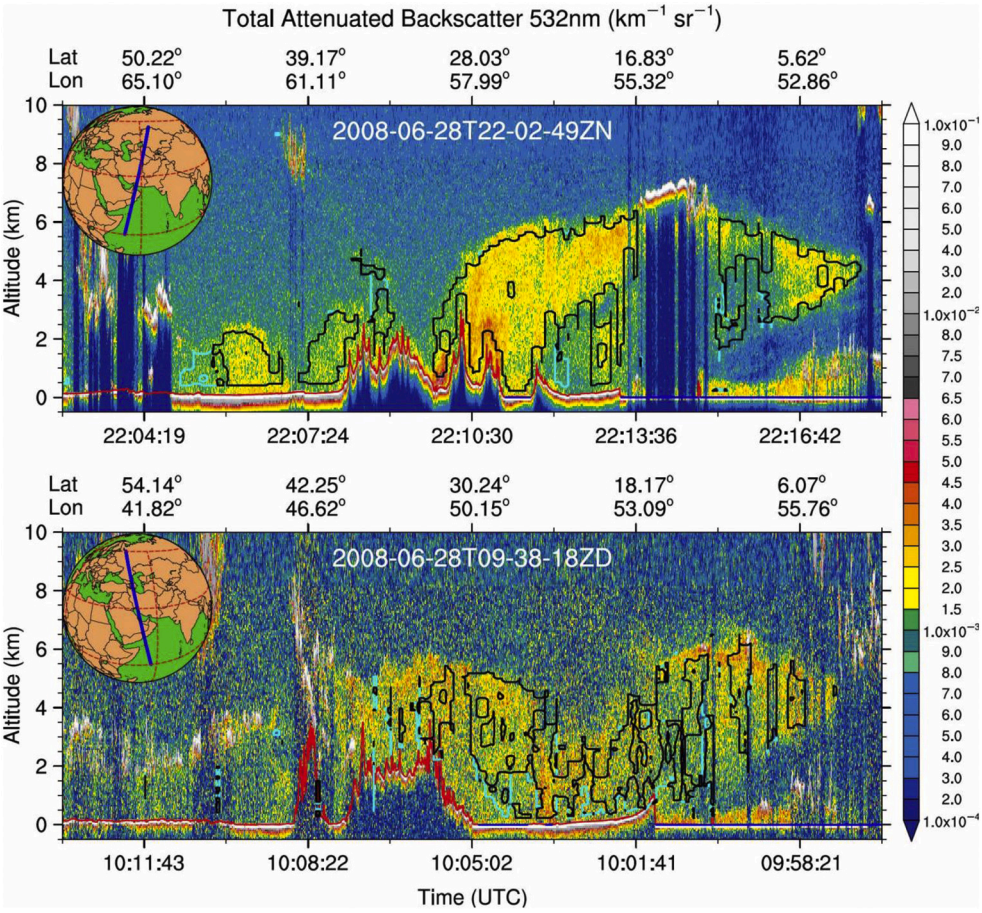


Fig. 7. Cross-section of aerosol attenuated backscatter (km^{-1} sr^{-1}) at 532 nm from CALIOP (Cloud-Aerosol Lidar with Orthogonal Polarization) on June 28, 2008. Top and bottom panels respectively show the nighttime and daytime observations. Bottom and top x-axes indicate the UTC (Coordinated Universal Time) time and the corresponding latitude and longitude; y-axis shows the altitude (km). The black and cyan contours indicate pure and polluted dust aerosols that are identified by the lidar depolarization ratio at 532 nm of 0.2 and 0.075, respectively (Li et al., 2010; Kim et al., 2018). The blue line on the map in the inset at the upper left corner in each panel demonstrates the corresponding track of CALIPSO (Cloud-Aerosol Lidar and Infrared Pathfinder Satellite Observation) satellite. The red and blue lines in the cross-section shows the altitude of the land and ocean surface, respectively. The horizontal and vertical resolution is 5 km along the track and 30 m, respectively. (For interpretation of the references to color in this figure legend, the reader is referred to the web version of this article.)

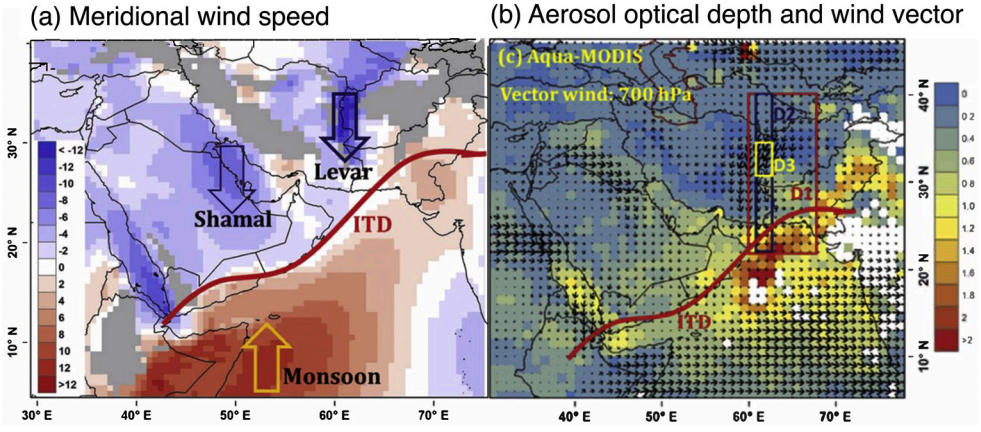


Fig. 8. (a) Meridional wind (shadings; units: m s^{-1}) at 850 hPa and (b) Aerosol optical depth (shadings) and wind (vectors; m s^{-1}) at 700 hPa during July 11–16, 2016. Data are from and MERRA-2 reanalysis and Aqua MODIS. The three boxes marked as "D1", "D2", "D3" in panel (b) represent dust source regions dominated by different Levar wind speed, with highest wind speed in D3, followed by D2, and D1. The area of near-zero meridional wind is defined as the Inter-Tropical Discontinuity (ITD) and indicated by the red line along the coastal line of the Arabian Peninsula, where dust aerosols tend to accumulate at a high altitude. Missing values of 850 hPa wind over high-altitude areas in panel (a) and aerosol optical depth in panel (b) are indicated by grey and white colors, respectively. July 2016 was a typical dusty month over the Arabian Sea with dust transported from various sources and along various pathways and thus was selected for the study. MODIS= Moderate Resolution Imaging Spectroradiometer (adapted from Rashki et al. (2019)). (For interpretation of the references to color in this figure legend, the reader is referred to the web version of this article.)

accompanied by the negative AOD anomalies of −0.2 to −0.6 (as departures from the 2000–2007 climatological mean) over the Arabian Sea (45°E–75°E; 10°N–27°N). This study showed that high (low) aerosol loadings over the Arabian Sea are closely related to the enhanced (reduced) ISM rainfall in July. However, due to relatively short data period and observation-based method in their study, a cause-effect relationship between aerosol loadings over the Arabian Sea and the ISM rainfall could not be concluded.

Using the method of multi-variate empirical orthogonal function (MV-EOF) and observation-based data, Jin et al. (2014) found a strong coupling among AOD over the Arabian Sea, mid and upper troposphere heating over the Iranian Plateau and the Arabian Sea, and the ISM circulation and rainfall. A correlation of 0.46 (p-value < 0.01) was found between AOD over the Arabian Sea and monsoonal rainfall over central and eastern India (20° N–32° N, 75° E–90° E) during June–July–August from 2000 to 2013. Here, the correlation coefficients between the ISM

rainfall and total AOD, DOD, and sea salt optical depth at each grid cell has been updated by extending the analysis period from 2000 to 2013 to 2000–2020 and employing multiple datasets for both aerosol and rainfall (Fig. 9). The correlations were calculated using monthly anomalies. The area-averaged ISM rainfall was positively correlated with satellite retrieved AOD and reanalysis assimilated DOD over the Arabian Sea, the southern Arabian Peninsula, and Iran and Afghanistan. Similarly, the area-averaged AOD and DOD are positively correlated with monsoon rainfall over the central and northern India, which is consistent with monsoon rainfall patterns in the MV-EOF analysis, as shown in Fig. 10a.

The physical mechanism behind such a correlation between dust and monsoon rainfall was examined using monthly composite analysis (Jin et al., 2014). It was showed that the high AOD anomalies over the Arabian Sea is coupled with strong atmosphere heating from the surface to 500 hPa over the Iranian Plateau and from 800 hPa to 600 hPa over the Arabian Sea, which strengthens the southwesterly monsoon winds. Finally, using daily data, they demonstrated that AOD over the Arabian Sea and the Iranian Plateau has a maximum correlation with ISM rainfall when AOD leads the rainfall by about 13 days.

3.3.2. *Modeled dust–monsoon relationship*

The foregoing positive correlation between dust and monsoon rainfall was further investigated in depth by a number of modeling studies. Using a general circulation model, Vinoj et al. (2014) found their model can well capture the spatial patterns of the observed correlation coefficients between the area-averaged monsoon rainfall (June–August) over central India (16.5° N–26.5° N, 74.5° E–86.6° E) and AOD over the Arabian Sea during 2000–2009. By removing dust, sea salt, anthropogenic emissions individually and in combination in their simulations, they further demonstrated that this observed dust–monsoon rainfall correlation can be attributed to radiative effects of dust and sea salt together, while anthropogenic aerosols do not play a role. Finally, based on dust pulse runs, they illustrated that when dust concentrations decrease from the beginning of the simulation, the monsoon rainfall starts to decrease on about the seventh day, indicating a lagged response of ISM rainfall to dust over Arabian sea in about one week.

One interesting result in the simulations by Vinoj et al. (2014) is that the monsoon rainfall has negative response to sea-salt aerosols over the Arabian Sea. Given an observed net positive correlation between monsoon rainfall and sea-salt optical depth (Fig. 9), their study strongly implies that the positive response of sea-salt emissions to monsoon circulations overwhelms the negative response of monsoon rainfall to sea-salt emissions. On the other hand, given an observed net positive correlation between dust and monsoonal rainfall (to the south of 20° N over the Indian Subcontinent) as well as a simulated positive monsoon rainfall response in South India to dust aerosols (Fig. 10), whether monsoon circulations increase or decrease dust emissions over the Middle East cannot be concluded based on their simulations. It is pertinent to note here that sea salt aerosols can interact with warm clouds by acting as Giant Cloud Condensation Nuclei (GCCN) and thus increase the efficiency of collision coalescence of cloud droplets and cause intense monsoonal rainfall over Western Ghats of India, where concentrations of sea salt are high due to strong monsoon circulations over the Arabian Sea, consequently exerting a positive impact on the ISM rainfall (Gerber and Frick, 2012; Konwar et al., 2012; Kumar et al., 2013). However, the possible interplays among feedback processes

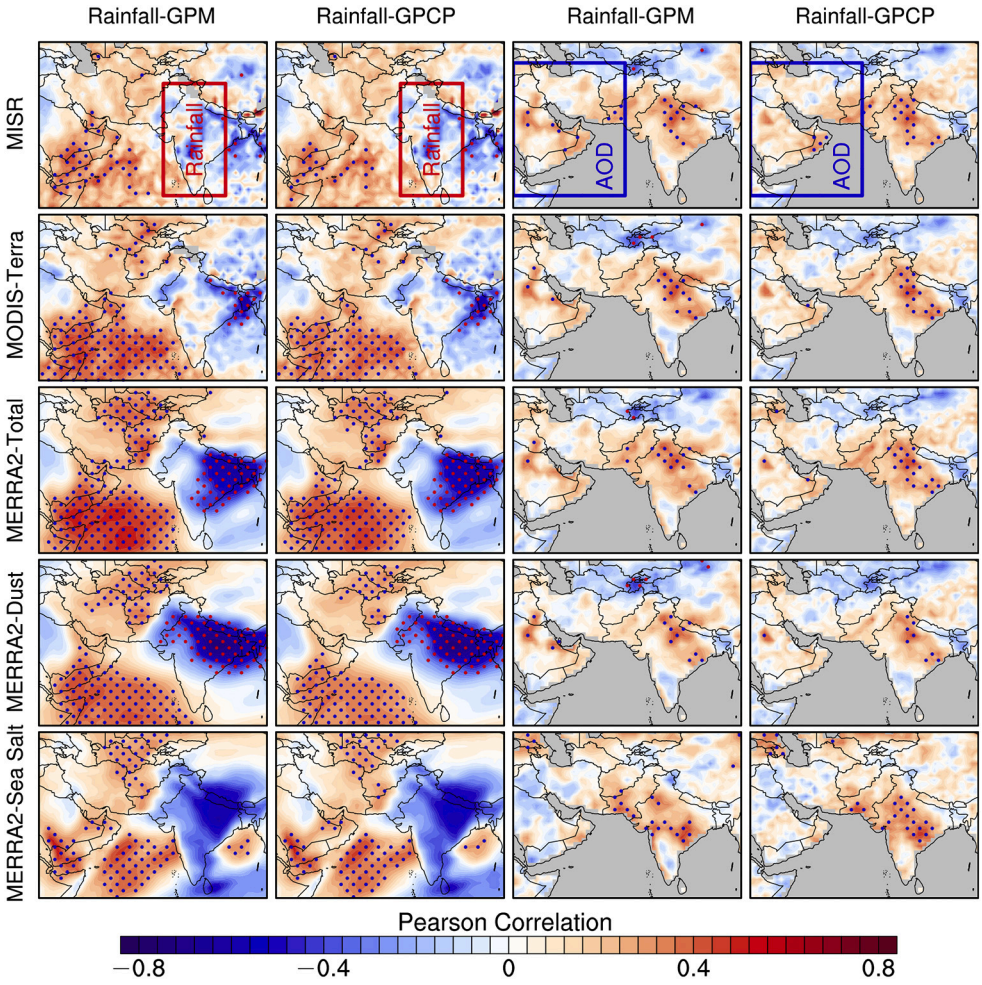


Fig. 9. The Pearson linear correlation coefficients between AOD and the ISM rainfall. The correlation coefficients are calculated using 80 (June–July–August–September) monthly anomalies from 2000 to 2019. Left two columns: correlation between area-averaged rainfall anomalies (GPM (first column) and GPCP (second column)) over India (land grid points in the red box: 8° N–35° N, 70° E–85° E) and the anomalies of total AOD (first three rows), MERRA2 dust AOD (fourth row), and MERRA2 sea salt AOD (fifth row) at each grid point. Right two columns: correlation between area-averaged anomalies of total AOD (first three rows), MERRA2 dust AOD (fourth row), and MERRA2 sea salt AOD (fifth row) over the Middle East and the Arabian Sea (blue box: 8° N–40° N, 40° E–67° E) and the anomalies of rainfall from GPM (third column) and GPCP (forth column) at each grid point. The grey colors represent missing values. Correlations significant at the 95% confidence level are dotted, with blue dots for positive correlations (red shading) and red dots for negative correlations (blue shading). GPM=Global Precipitation Measurement; GPCP=Global Precipitation Climatology Project. (For interpretation of the references to color in this figure legend, the reader is referred to the web version of this article.)

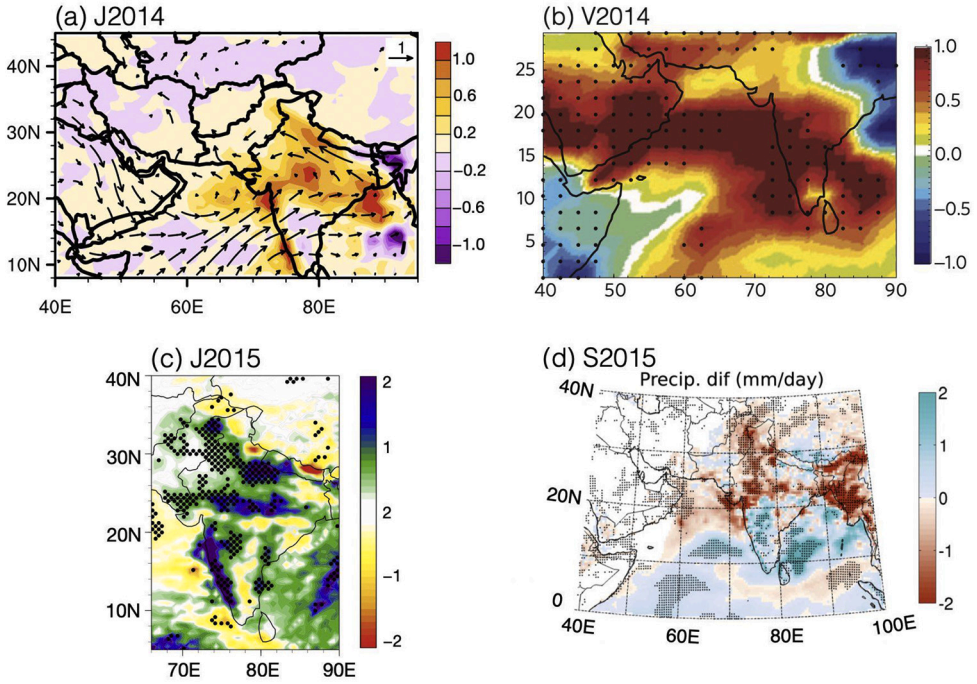


Fig. 10. Comparison of the dust–monsoon rainfall relationship in four studies. (a) An observational study showed a positively coupled relationship among the normalized values of the Middle East dust, monsoon circulation at 850 hPa, and rainfall, which was based on a multivariate empirical orthogonal function (MV-EOF) analysis using data from 2000 to 2013 (Jin et al., 2014). Simulated monsoon rainfall (mm day^{-1}) response to dust aerosols in (b) the Community Atmosphere Model (CAM5) over June–August for 10 years equilibrium simulations (Vinoj et al., 2014), (c) a regional weather forecasting model (WRF-Chem) over June–August for 2008 (Jin et al., 2015), and (d) a regional climate model (RegCM4) over the period of June–September for 2000–2009 (Solmon et al., 2015). Black dots in panels (b)–(d) indicate grid cells with statistically significant monsoon rainfall responses (Adapted from Jin et al. (2014); Vinoj et al. (2014); Jin et al. (2015); Solmon et al. (2015)).

induced by dust and sea salt are not well understood and need to be further investigated in the future.

Using a regional climate model–the Weather Research and Forecasting model coupled with online Chemistry (WRF-Chem), Jin et al. (2015) performed an ensemble of simulations of high resolution (54 km) in the summer (June–July–August) of 2008 to reexamine in detail the physical mechanism behind the dust–monsoon correlation. They designed 32 ensemble simulations by employing various physical and chemical schemes, such as planetary boundary layer, aerosol mixing states, aerosol optical calculation methods, to reduce model uncertainties and retrieve statistically meaningful results. By comparing the difference of the ensemble means of simulations with and without dust emissions, they found that the ISM monsoon rainfall has statistically significant response to the dust aerosols. The area-averaged monsoon rainfall over the whole India (20°–32° N, 70°–85° E) increased by 0.44±0.39 mm day^{-1} (mean and standard deviation based on ensemble members), which accounted for about 10% of the climatology. The spatial patterns of rainfall response are well captured: with increased rainfall along the southwest coastal India and in the regions to the north of 20° N in the Indian subcontinent (Fig. 10). Such a spatial pattern was corroborated by a recent modeling study (Rahimi et al., 2019). Further analyses of model results indicate that dust aerosols can heat the atmosphere from 900 to 500 hPa with the maximum around 600 hPa over the Arabian Sea. This heating could cause a pressure low at 850 hPa centered over the Arabian Sea that strengthens southwesterly monsoon flow, which in turn transports more moisture from the Arabian Sea to the Indian subcontinent (Fig. 11a) and results in increases in moist static energy and rainfall over India (Fig. 11b). Moreover, the model indicated a maximum and statistically significant correlation coefficient of 0.4 when AOD leads the monsoon rainfall by 11 days, which is very close to 13 days retrieved in observations (Jin et al., 2014).

The above two model simulations include a very large domain, within which there are several large dust source regions. To quantify and

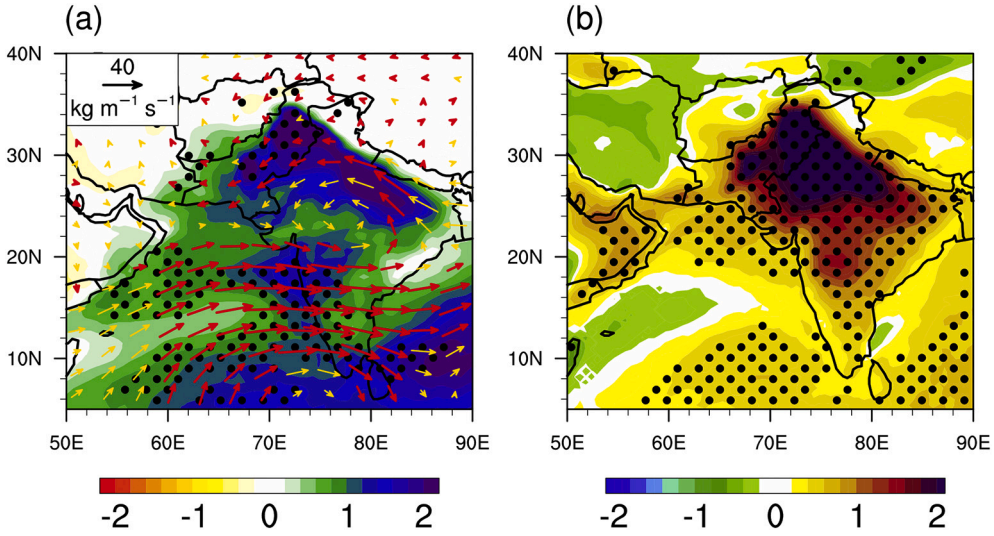


Fig. 11. Simulated differences between the dust and non-dust experiments for (a) precipitable water (shading; unit: mm) and water vapor flux (arrows; units: kg m^{-1} s^{-1}) both integrated within the entire atmospheric column and (b) moist static energy (units: kJ kg^{-1}) in the three lowest model layers. Black dots represent the differences that are statistically significant at 95% confidence level based on a one-sided Student's t test. The red arrows represent wind differences that have a 95% confidence level, and the gold arrows represent non-significant wind differences. The simulations covered June–July–August in 2008 using the Weather Research and Forecasting model with online coupled chemistry (WRF-Chem) (copied from Jin et al. (2015)). (For interpretation of the references to color in this figure legend, the reader is referred to the web version of this article.)

compare the monsoon rainfall responses to each dust source region and anthropogenic emissions in South Asia, Jin et al. (2016b) selected three main dust source regions—the Middle East, the Thar Desert along the border between India and Pakistan, the Taklimakan and Gobi Deserts in West China, and designed simulations with dust emissions set to zero in each of these deserts. The difference between each of these simulations from the control simulation which included dust emissions in all deserts represent the impact of each individual desert on the monsoon rainfall. They found that the Middle East dust aerosols contribute to 77% of total increases in the monsoon rainfall induced by dust aerosols in the whole domain, which is comparable to the anthropogenic emission-induced contribution (i.e., 70% of the total rainfall increases due to dust).

Dust aerosols also affect ISM variability on intraseasonal and interannual timescales. The intraseasonal variability of the ISM rainfall can be attributed to synoptic events, such as cyclones, depressions, and thunderstorms. A better understanding of the factors that contribute to the intraseasonal variability could significantly improve the predictability of the ISM rainfall (Hazra et al., 2013a; Hazra et al., 2013b; Saha et al., 2019; Saha et al., 2020; Swenson et al., 2020). Using satellite dataset, Singh et al. (2015) demonstrated that the dust and anthropogenic aerosols over the Indian subcontinent could modulate the intraseasonal variability of the ISM rainfall through altering cloud microphysical properties. A modeling study further found that dust aerosols from the Middle East could increase the amplitudes of the intraseasonal oscillations (ISOs) of the ISM rainfall with 10–20 and 30–60 day periodicities and also substantially enhance the spatial variability of the 10–20 days ISOs (Singh et al., 2019). The impact of dust aerosols on the interannual variability of ISM rainfall was studied by Solmon et al. (2015) with a set of ten year simulations from 2000 to 2009. They found that when dust emissions were prescribed as an increasing trend similar to that estimated using satellite retrieved AOD, the model can capture the observed increasing trend in monsoon rainfall during 2000–2009 (Fig. 10). However, when dust emissions were not prescribed and thus no trend in simulated AOD, the model failed to capture the increasing trend in monsoon rainfall. Their results indicate that the dust–monsoon relationship also exists on the decadal timescale. Note that the reason to prescribe dust emissions in their model simulations is that most of the current climate models cannot capture the interannual variability or long-term trend of dust emissions (Evan et al., 2014; Evan, 2018). Therefore, one drawback of their study is that there is no feedback from monsoon on dust emissions, which will be discussed in more detail in Section 4.1.

3.3.3. Uncertainties in modeled dust–monsoon relationship

The spatial patterns of the ISM rainfall responses to the Middle East dust are very different in observation-based study (Jin et al., 2014) and numerical modeling studies (Vinoj et al., 2014; Solmon et al., 2015), as compared in Fig. 10, albeit all studies illustrated positive ISM rainfall response to the remote Middle East dust aerosols. The observation-based study showed that the positive monsoon anomalies due to dust are mainly confined to north of 20° N over the Indian subcontinent (Fig. 10a), while the modeling studies showed that the dust-induced positive rainfall anomalies are mainly located south of 20° N (Fig. 10b and d). Moreover, Jin et al. (2014) found a dust–monsoon interaction timescale of approximately 2 weeks, which is much longer than 5–7 days concluded from model simulations by Vinoj et al. (2014). Potential reasons for the spatial and temporal discrepancies in dust-induced monsoon rainfall changes among the foregoing studies are (1) the relatively coarse spatial resolution of the general circulation model (1.9° latitude × 2.5° longitude) used by Vinoj et al. (2014); simulations of high spatial resolution (about half degree) have been shown to be necessary to resolve the complex topography of the Tibetan Plateau (i.e., sharp gradient of altitude), which could largely improve the model performance in South Asia (Duan et al., 2013; Lin et al., 2018). (2) Uncertainties in model parameterizations of dust-related physical and optical processes. For example, modelled dust direct radiative effect demonstrates significant sensitivities to various shortwave radiation schemes (Fountoukis et al., 2018), planetary boundary layer schemes (Alizadeh Choobari et al., 2012), and assumptions of the dust mixing states with other aerosol species (Sokolik et al., 2001; Tuccella et al., 2020).

To reduce these two model uncertainties, Jin et al. (2015) designed 32 ensemble simulations of high spatial resolution (54 km) by employing various schemes of planetary boundary layer, shortwave radiation, and aerosol mixing state. The ensemble means of the dust-induced monsoon rainfall changes manifested very similar spatial patterns to those in the observational study (Fig. 10a versus Fig. 10c). It is worth mentioning that the spatial correlations between the modelled and observationally regressed monsoon rainfall response to the Middle East dust aerosols show a wide range (−0.05 to 0.5) across various ensemble members (Jin et al., 2015), implying the importance of ensemble simulations in improving the model performance in capturing the complex of dust–monsoon interactions.

The magnitude and sign of the simulated ISM rainfall response to the Middle East dust are determined by the parameterization of dust absorbing properties. Dust absorbing ability is parameterized by the imaginary part of its complex refractive index, which spans a considerably diverse range from 0.001 to 0.008 in various climate models (Jin et al., 2016a; Di Biagio et al., 2019b). Model sensitivity study manifested that as dust aerosols change from purely scattering to highly absorptive (i.e., the imaginary part of dust refractive indices ranges from 0 to 0.008), the dust-induced monsoon rainfall increases from −0.2 to 1 mm day^{-1} (Jin et al., 2016a), with a sensitivity of +0.16 (mm day^{-1}) per ($i \times 10^{-3}$), as shown in Fig. 12. By comparing model results against observational composite analysis, they found that monsoon rainfall response to dust aerosols is underestimated in their simulations, indicating more absorptive dust aerosols over the Arabian Sea may be needed to increase realism of the simulations.

3.4. Impact of dust–cloud interaction on the ISM

Besides the foregoing dust–radiation interaction, dust aerosols can also modulate the ISM system through dust–cloud interaction. Dust aerosols interact with cloud by acting as cloud condensation nuclei (CCN) and ice nuclei (IN), which can alter cloud microphysics, brightness, lifetime, cloud area cover, and consequently precipitation (Rosenfeld et al., 2001; Chen et al., 2008; Karydis et al., 2011; Nenes et al., 2014; Karydis et al., 2017; Jha et al., 2018). Pure mineral dust aerosols comprise a large portion of insoluble minerals and thus are not efficient CCN (Sullivan et al., 2009; Murray et al., 2012), but they can be coated by sulfate and nitrate and become efficient CCN through heterogeneous reactions with sulfur dioxide and nitrogen oxides during their transport in the troposphere (Trochkine et al., 2003; Levin and Cotton, 2008; Li and Shao, 2009; Matsuki et al., 2010). Dust aerosols may exert two contrasting effects on clouds once activated depending on their size distributions: (1) a large concentration of small dust particles (with radii $< \sim 1$ μm) could result in the formation of small cloud droplets and thus low coalescence efficiencies and less or delayed precipitation (e.g., Rosenfeld et al., 2001); (2) the large dust particles (with radii $> \sim 1$ μm) may act as giant CCN and result in high coalescence efficiencies and consequently facilitate precipitation (e.g., Kelly et al., 2007). Dust is also one of the most important sources of IN in mixed-phase and cirrus clouds (DeMott et al., 2003; Pratt et al., 2009; Kamphus et al., 2010; Baustian et al., 2012; Creamean et al., 2013; Cziczo et al., 2013; Tobo et al., 2019). Adding IN in a supercooled liquid cloud could increase the hydrometeor size, reduce hydrometeor concentration, and increase precipitation (Andreae et al., 2004; Lohmann and Feichter, 2005; Rosenfeld, 2006; Rosenfeld et al., 2008). Our understanding about dust acting as IN remains poorer than dust as CCN, largely due to our limited knowledge about what makes efficient IN.

Although a growing number of studies have investigated the dust–cloud interactions, studies about dust–cloud–ISM rainfall interactions

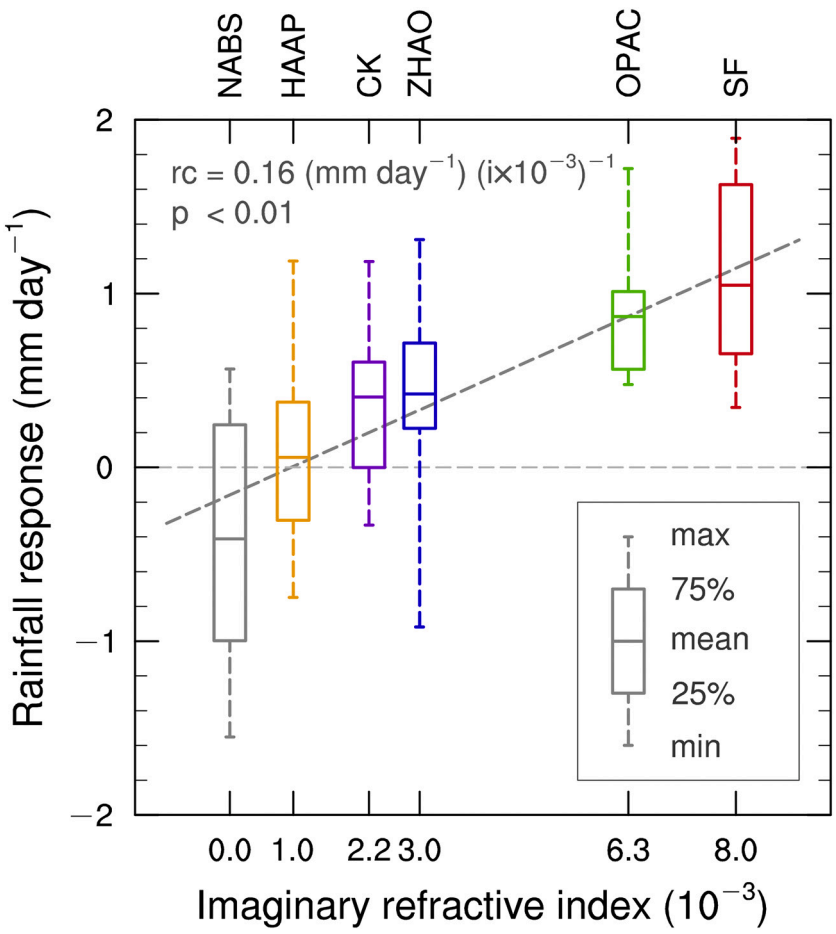


Fig. 12. The simulated dependence of the response of Indian summer monsoon rainfall (8°–35° N, 70°–85° E) to the Middle East dust aerosols on dust absorbing property parameterized by the imaginary refractive index of dust. The period is for June–July–August in 2008. The dash line represents the least squares linear regressed from the means of rainfall responses on dust imaginary refractive indices (copied from Jin et al. (2016a)).

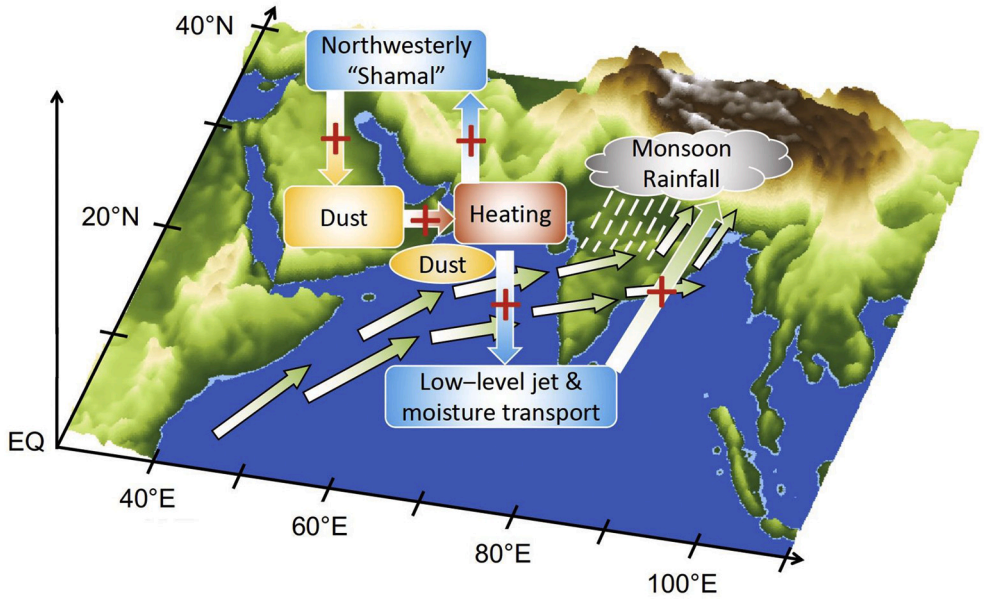


Fig. 13. A schematic showing how the Middle East dust aerosols influence the ISM rainfall through the dust–radiation interaction. Red plus signs represent positive responses. "EQ" stands for equator (modified from Jin et al. (2015)). (For interpretation of the references to color in this figure legend, the reader is referred to the web version of this article.)

are limited. Recently, using multiple satellite observations (e.g., CALIPSO and MODIS) and reanalysis data, (Patel et al., 2019) investigated dust-induced changes in ice cloud properties and precipitation over the ISM region. They found contrasting dust-induced changes in ice cloud depending on cloud regimes: (1) For thin ice clouds, dust induced a 25% reduction in ice particle radius; (2) for thick ice clouds in strong updraft regimes, dust induced a 40% increase in ice particle radius and ice water path, which resulted in cloud deepening (so-called cloud invigoration effect) and consequently strengthened precipitation susceptibility. In light of high concentrations of dust aerosols and their significant impacts on clouds and monsoonal rainfall (Chen et al., 2008; Nenes et al., 2014), more effort should be put on the dust–cloud–ISM rainfall interactions in future.

3.5. Summary of dust impacts on monsoon

Two physical mechanisms through which the dust aerosols emitted from the Arabian Peninsula influence the ISM system are proposed: dust–radiation and dust–cloud interactions. The dust–radiation mechanism is summarized in a schematic in Fig. 13. The northwesterly "Shamal" winds reach its peak in the boreal summer and lift abundant quantities of dust particles in the atmosphere from major deserts in the Arabian Peninsula. These dust particles can be readily transported southeastward over to the Arabian Sea, where the confluence of the northwesterly Shamal winds and the strong southwesterly summer monsoon flow cause strong uplift and thus accumulation of dust aerosols within 900–500 hPa atmospheric layers. The elevated dust aerosols over the Arabian Sea can heat the lower and middle troposphere by their strong absorption of solar radiation and deepen the strong north-south thermal gradient, which further strengthens both the southwesterly monsoon flow and the northwesterly Shamal winds. The enhanced southwesterly monsoon flow could transport more water vapor from the Arabian Sea to the Indian subcontinent and consequently cause an increase in monsoon rainfall. On the other hand, the enhanced northwesterly Shamal winds could generate and transport more dust particles from the Arabian Peninsula to the Arabian Sea, and thus forming a positive feedback loop between dust and Shamal winds. The higher terrain of the Iranian Plateau and the western Himalayas can enhance the accumulation of dust over the foothill regions and the rising motion of air (Lau et al., 2020). Such a physical mechanism linking dust heating and the enhanced low-level southwesterly over the Arabian Sea leading to increase ISM rainfall in downwind regions is analogous to the EHP effect over the Tibetan Plateau (Lau et al., 2006). The dust–cloud mechanism works mainly through dust aerosols acting as ice nuclei, which can alter the microphysical properties of ice clouds and consequently the ISM rainfall (Patel et al., 2019).

4. The ISM impact on dust emission and transport

4.1. The ISM impact on Arabian dust emission

It has long been recognized that the global monsoon systems can cause desertification in subtropical regions. The monsoon diabatic heating can induce Gill-Matsuno-type Rossby waves (Matsuno, 1966; Gill, 1980) that propagate westward and causes the southern flank of the midlatitude westerlies to descend and consequently form global major deserts (Rodwell and Hoskins, 1996, 2001; Tyrlis et al., 2012; Tyrlis et al., 2014). Through the above mechanism, the ISM could significantly influence the summertime circulation over the Arabian Peninsula and adjoining regions at inter-annual timescale (Attada et al., 2018). During the strong ISMs, the upper tropospheric heating induced by latent heat release in strong monsoonal convections expands westward over the northern Arabian Peninsula. This expansion of heating triggers the Rossby wave that is forced westward by the upper tropical easterly jet. The westward expansion of the upper-tropospheric high strengthens the upper-level convergence and mid- to low-level divergence, resulting in a low-level high pressure centered over the northern Arabian Peninsula. The low-level high pressure strengthens the north to south pressure gradient and thus the northwesterly Shamal wind. This hypothesis is depicted as a schematic diagram in Fig. 14. Note that this low-level high pressure could also prohibit the formation of clouds and precipitation and thus may result in drier soil and enhance dust emissions. Although the mechanism through which the ISM could module the Arabian Peninsula summertime climate has been proposed, few studies have explored the extent to which the ISM can influence dust emissions over the Arabian Peninsula through perturbing circulations and surface soil properties.

4.2. The IMS impact on dust horizontal transport to the Arabian Sea

Not until a recent study from Sharma and Miller (2017) that addressed the potential impact of the ISM circulation on dust emissions in the Arabian Peninsula, have almost all of the previous studies focused on dust aerosols' impact on the ISM rainfall. By omitting the radiative effect of dust aerosols in their simulations, they addressed how the ISM influences dust emissions in the Middle East and the Arabian Sea. After turning off dust radiative effect, they can still detect statistically significant positive correlation between monsoon rainfall over central India and AOD over the Arabian Sea. Therefore, they attributed the observed dust–monsoon correlation to the impacts of monsoonal winds on dust emissions and transport from the Arabian Peninsula to the Arabian Sea instead of dust radiative effect on monsoon rainfall. However, the simulated positive correlation between AOD and monsoon rainfall could also come from the positive correlation between monsoon circulation and sea salt aerosols given that the southwesterly monsoon winds is the main driver of the sea salt emission over the Arabian Sea (Li and Ramanathan, 2002; Vinoj and Satheesh, 2003; Vinoj et al., 2014). Such a positive correlation between the ISM rainfall and sea-salt can also be detected in reanalysis data, as shown in Fig. 9. We believe that it warrants a more stringent model experiment design, in which the interaction between sea-salt and the ISM system should be removed by turning off sea-salt emission in model simulations. to address the physical mechanisms behind the dust–monsoon interaction in the future.

4.3. The ISM impact on dust vertical transport to upper troposphere and lower stratosphere (UTLS)

Strong overshooting deep convection associated with the ISM system can efficiently transport dust aerosols among other air pollutants from surface to the UTLS (Randel et al., 2010; Yu et al., 2017). During the ISM onset, dust aerosols emitted from the Thar Desert and Arabian Peninsula start to be transported to the Indo-Gangetic Plain by the strong low-level monsoon southwesterly and then get trapped by local topography and accumulated over this region (Xu et al., 2018; Hu et al., 2019; Hu et al., 2020). Fine dust particles in the upper troposphere and lower stratosphere above clouds where wet scavenging is minimized, can reach a highest concentration during peak monsoon season due to strong vertical transport by penetrative deep convections. It has been suggested that monsoonal overshooting deep convections play crucial roles in uplifting dusts from the Middle East and adjacent desert regions, as well as and other pollutants in the Asian Summer Monsoon (ASM) regions into the UTLS through preferred pathways along the Himalayas foothills around the western, southern and eastern edge of the Tibetan Plateau (Lau et al., 2018; Yuan et al., 2019).

5. Alternative hypotheses on dust–monsoon relationship

5.1. Topographic heating over the Iranian Plateau

The dust–monsoon relationship has been relatively well addressed from the weekly to seasonal timescales but has not been systematically

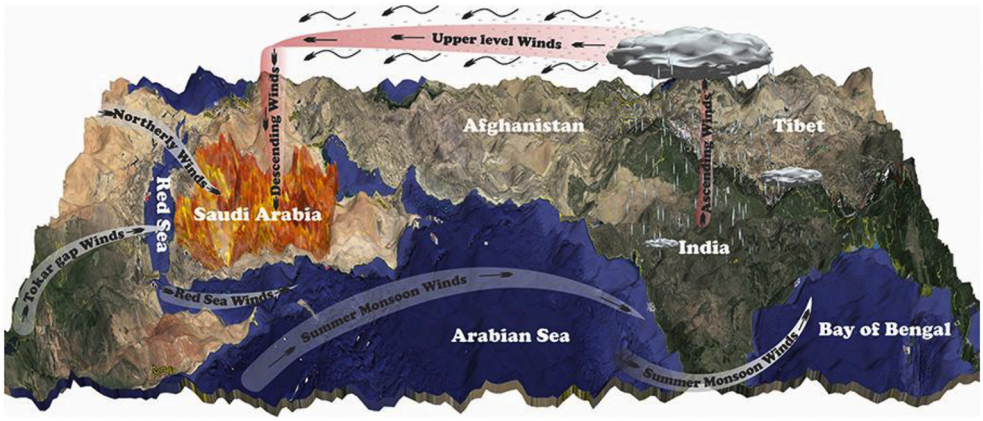


Fig. 14. A schematic diagram showing how the Indian summer monsoon cloud influence the Arabian Peninsula summertime climate. The monsoon-induced upper tropospheric heating expanded westward and reached a maximum over the northern Arabian Peninsula during strong monsoons. This heating may trigger the Rossby wave that is pushed westward by the upper tropical easterly jet. The westward expansion of the upper-tropospheric high intensified the mid- to low-level divergence over the Arabian Peninsula, which could cause a near-surface high pressure and consequently influence the summertime climate over the Arabian Peninsula, such as resulting in a strengthened northwesterly Shamal wind (Attada et al., 2018) (copied from KAUST (2018)).

studied from the decadal to interdecadal timescales due to a lack of long-term satellite observations of dust emissions. Using wind data as a proxy for dust emissions, Jin (2015) investigated the interdecadal variabilities of the Arabian dust and the ISM rainfall from 1979 to 2013. Here, we have extended the time period to 1980–2019 and evaluated the robustness of the interdecadal variabilities by employing multiple datasets of rainfall and wind. The frequency and magnitude of strong winds were used as a proxy of dust emissions since satellite retrievals of aerosol optical depth were not available over the Arabian Peninsula before 2000. Strong winds were defined as hourly wind speeds that are greater than the 90th local percentiles, which was calculated for each month using hourly data from 1980 to 2019. The results showed positive trends during the period of 2002–2019 in both the frequency and magnitude of the strong winds in MERRA reanalysis and AOD in three satellite retrievals over the Arabian Peninsula, as well as the ensemble mean of the ISM rainfall in three rainfall datasets over the Northern Central India (Fig. 15). From 1980 to 2001, however, negative trends were detected in the ISM rainfall and the strong wind frequency and magnitude in MERRA. These preliminary results suggested that the Arabian dust could interact with the ISM system at the interdecadal timescale. Note that no significant trends in strong wind frequency and magnitude were detected in MERRA-2 reanalysis during the period of 1980–2001, but similar positive trends were seen in MERRA and MERRA-2 during the period of 2002–2019. The differences in the MERRA and MERRA-2 wind fields were also seen over North Africa (Evan, 2018). Attribution of the differences is beyond the scope of this review.

One possible physical mechanism linking the Arabian dust and the

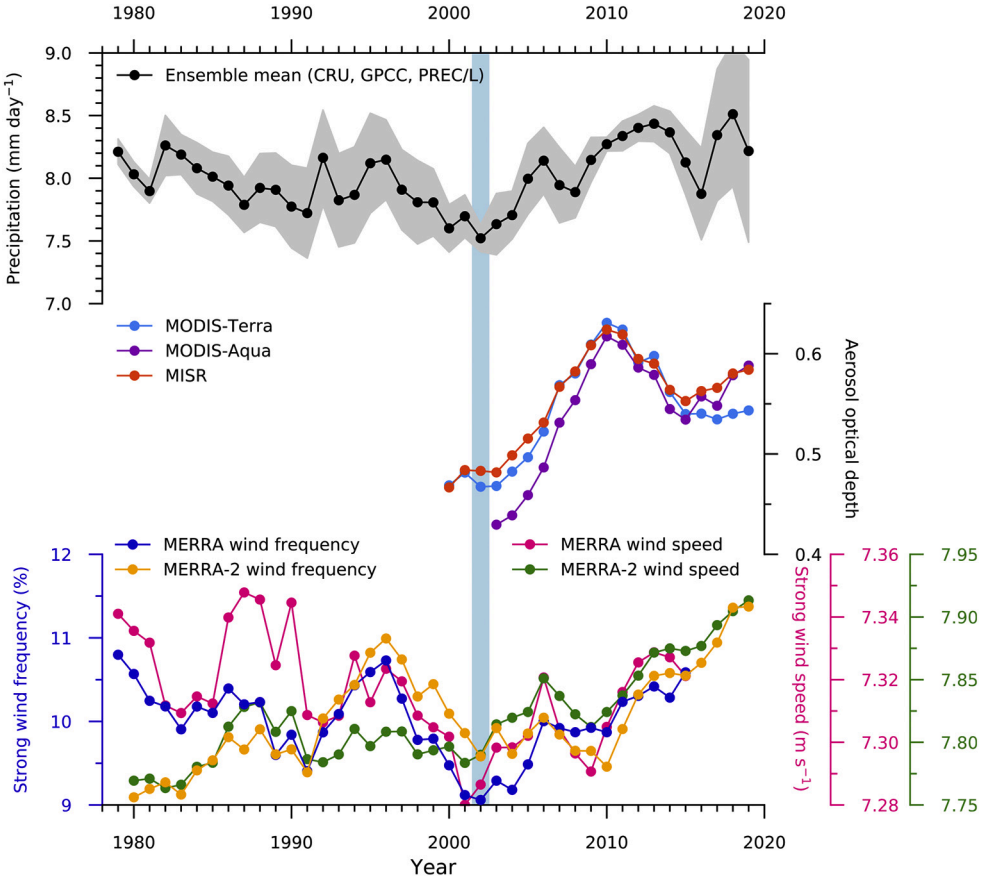


Fig. 15. Decadal dust–monsoon relationships. The ensemble mean monsoon precipitation rate (mm day^{-1}) is area-averaged over North Central India during June–July–August–September. Three precipitation datasets–CRU, GPCC, and PREC/L, are used to calculate the ensemble mean and the gray area indicates one standard deviation of the three datasets. Aerosol optical depth and strong wind frequency (%) and speed (m s^{-1}) are area-averaged over South Arabian Peninsula during the boreal summer (i.e., June–July–August). Strong winds are defined as hourly wind speed greater than the 90th percentile of local wind. The vertical bar marks the reversal of these variables around 2002.

ISM rainfall at the interdecadal timescale is through the thermal forcing of the Iranian Plateau. The summertime temperature in the mid-troposphere over the Iranian Plateau was found to be positively correlated with 1) the ISM rainfall at the interdecadal timescale from 1967 to 2015 (Zhang et al., 2019b) and 2) the summertime near-surface Shamal wind and AOD over the Arabian Peninsula and the Arabian Sea from 2000 to 2013 (Jin et al., 2014). Therefore, here we propose another hypothesis that the observed positive dust–monsoon correlation could be partially attributed to the heating over the Iranian Plateau, which could enhance the dust emissions over the Arabian Peninsula through strengthening the Shamal winds as well as the ISM circulations and rainfall at the interdecadal timescale. Numerous factors could contribute to the mid-troposphere temperature variations over the Iranian Plateau, and further studies are needed to identify them. However, it is worth mentioning that dust and soil moisture are two potential factors that can influence the mid-troposphere temperature over the Iranian Plateau.

5.2. Cloud-radiation-circulation feedback

Recent climate model experiments have indicated that the impacts of Middle East dust, through radiation-circulation interactions, are likely to extend from the ISM to the East Asian summer monsoon (EASM), and regions beyond. Numerical experiments performed using the Model for Prediction Across Scales (MPAS) coupled with the Community Atmosphere Model (CAM5) physics shows that increased dust emissions and transport from the Middle East/West Asia region induces a strong dust-cloud-radiation-circulation feedback, resulting in warmer and moister troposphere with enhanced cloudiness and precipitation over the Pakistan/Northwest India (PNWI) region (Lau et al., 2020). The warming is amplified by the dust induced Elevated Heat Pump (EHP) mechanism along the West Himalayas/Iranian Plateau foothill regions, most pronounced during May–June. During July–August, cloud–radiation–circulation feedback further enhances the warming of troposphere over the PNWI and adjacent regions over West Asia, as well as induced cooling over East Asia. The upper tropospheric heating and increased precipitation over PNWI spur a large-scale anomalous Rossby wave train and a northward displacement of the subtropical jet stream, accompanied by a westward shift of the Western Pacific Subtropical High. As a result, the entire ASM precipitation-cloud system is displaced westward. Precipitation and cloudiness are intensified over northwest and western India and West Asia but suppressed over southern and central East Asia. The simulated responses of precipitation and cloudiness to the dust-induced westward shift of the WPSH and entire ASM system are generally consistent with observational studies. Observations demonstrated that a westward shift of the monsoon trough over South Asia and the North Pacific Subtropical High is associated with an enhancement in precipitation over PNWI and East Asia (Mujumdar et al., 2012; Preethi et al., 2016). Analyses of the sub-seasonal to seasonal variability of the upper-level vorticity balance suggests that anomalous diabatic heating over PNWI induced by Middle East dust radiative heating plays an important role in anchoring a quasi-stationary upper level Rossby wave train spanning Eurasia, the Tibetan Plateau/northern India, and East Asia, affecting the regional climate of these regions.

While the aforementioned idealized climate model experiments have offered plausible mechanisms for extended influence of the Middle East dust on ASM variability, details of the regional feedback processes are subject to uncertainties in model representation of physical and optical properties of dust aerosols, as well as the physics of dust emissions, transport and removal processes. These mechanisms, and possibly others, need to be better understood and validated against available observation records of dust aerosols, clouds, impurities in snow and meteorological variables from re-analyses, as well as multi-model intercomparison studies.

6. Challenges in dust simulation and global implications

6.1. Dust interannual and decadal variabilities in simulation

Global and regional dust emissions demonstrate strong interannual and decadal variabilities (Mahowald et al., 2010; Zhang and Reid, 2010; Hsu et al., 2012; Shao et al., 2013; Evan et al., 2016; Klingmüller et al., 2016; Pu and Ginoux, 2016; Jin et al., 2018; Gandham et al., 2020). Many studies on dust–climate interactions focused on the seasonal or shorter time scale, largely because current climate models, including both regional and global models, are unable to capture the observed interannual or decadal variability of dust emissions. Evan et al. (2014) compared African dust emissions in 23 CMIP5 model simulations against satellite retrievals for 1982–2005 and found that all simulations significantly underestimated dust loadings and failed to capture the observed dust interannual variability. Smith et al. (2017) found that the correlation coefficients between the simulated dust by CESM and observations for the period of 1990–2005 ranged from 0.1 to 0.6 in global major dust source regions, indicating that the model still have difficulty in accurately simulating interannual variability in dust.

To produce more realistic dust emissions in climate model simulations comparable to satellite retrievals, modelers have to adjust the tuning factor in dust emissions scheme or the dust erodibility map in the model input data for each season or each year. For example, using a regional climate model of high horizontal resolution, Solmon et al. (2015) found that the model cannot reproduce an observed increasing trend of AOD over the Arabian Peninsula during 2000–2009. To reproduce such an increasing trend in the model, they had to prescribe dust emissions in the erodibility maps. However, prescribing dust emissions can result in the lack of meteorological feedback to dust emissions, which was shown to play an important role in dust emissions and transport (Sharma and Miller, 2017). Therefore, this method is not suitable to study the two-way interactions between dust aerosols and climate. Note that even for simulations of dust storm events, the emission rates have to be adjusted for each event, because they are highly case-dependent and can span a wide range from 0.65 to 22 $\mu g\ s^2\ m^{-5}$ in different dust source regions and during different seasons (Kim et al., 2017). It is also worth pointing out that the use of the tuning factor used in most of dust emission schemes is to scale the magnitude of dust emissions so that the simulated total AOD is comparable to satellite retrieved values or other observations, but there is no physical basis for the tuning. As a result, although the tuning factor plays an important role in simulating dust emissions, it is not influenced by meteorological fields and thus reduces the susceptibility of dust emissions to climate change.

Recently, a temporally dynamic soil erodibility map that is highly susceptible to wind speed was developed and evaluated against surface observations. By combining theory, observations, and numerical simulations, (Kok et al., 2014b) derived a physically based dust emission parameterization, in which a dynamic dust emission coefficient that is a measure of soil erodibility was introduced. The dust emission coefficient has similar spatial patterns to dust source functions developed in previous studies (e.g., Ginoux et al., 2001), but it is calculated based on the standardized threshold friction velocity and thus it is time varying. Model results shown that the new dust emission scheme is sensitive to climate change and can significantly improve the simulation of the spatial patterns of dust emissions (Kok et al., 2014a). However, preliminary investigations showed that the new dust emission scheme has a limited ability to capture the interannual variability of dust optical depth over the dust-dominated region of 10–20°N and 20–30°W, off the West-African coast from 1980 to 2008, albeit it better reproduced the long-term trend of dust optical depth (Kok et al., 2018). More modeling studies should be carried out to assess the ability of the new dust emission scheme in reproducing the interannual variability of dust emissions in major dust source regions across the globe.

Besides dust emissions, there are still a number of other factors that

could cause biased simulations of dust interannual variability, such as near-surface wind speed and land surface properties (Pu and Ginoux, 2017; Evan, 2018; Jin and Wang, 2018; Pu et al., 2019; Pu et al., 2020). However, very few studies have elucidated the causes of the systematic errors in interannual variability of dust emissions in model simulations. Using an idealized model, Evan (2018) showed that a biased dust interannual variability in CMIP5 models came from errors in surface winds rather than the representation of dust emission processes. Pu and Ginoux (2018) found that CMIP5 models tend to overestimate the influences of surface winds on dust emissions and underestimate the influences of vegetation in comparision with obsevations. Therefore, future studies should also be focused on the boundary layer processes to improve the simulation of near-surface wind speed and vegetation variations and ultimately dust interannual and decadal variabilities.

6.2. Factors affecting dust absorption of solar radiation

The climatic impacts of dust aerosols are mainly through absorbing solar radiation and heating the atmosphere, such as the Middle East dust–ISM interaction and the EHP effect over the Tibetan Plateau. Dust absorption is determined by multiple factors: particle number size distribution, chemical mixing state, complex refractive index, chemical compositions, particle shape, vertical distribution relative to clouds, and land surface reflectance under dust layer, among others. In this review, we address the uncertainties in the first three factors.

6.2.1. Size distribution

The size distribution of dust aerosols plays a dominant role following dust mass load in determining the direct radiative effects (Mahowald et al., 2014). Small dust particles (< 2 μm) exhibit strong scattering of solar radiation, while large dust particles (> 10 μm) demonstrate strong absorption of both solar and terrestrial radiation (Tegen and Lacis, 1996; Miller et al., 2006). Not until recently, has the scientific community considered the fact that a significant amount of dust particles suspended in the atmosphere over source regions and even transported long-range can readily reach sizes > 10 μm (Stuut and Prins, 2014; van der Does et al., 2018). A number of global climate models overestimate fine dust by a factor of 2–8 relative observations (Kok, 2011) yet underestimate coarse dust by a factor of 4 (Adebiyi and Kok, 2020), which caused an overestimation of dust cooling effect (Kok, 2011). With a corrected dust size distribution and dust abundance load, the globally averaged dust direct radiative effect was estimated between −0.48 to +0.20 W m^{-2} that was a much less cooling effect than the ~−0.4 W m^{-2} estimated by current global climate models (Kok et al., 2017; Kok et al., 2018). These results imply that dust aerosols may play a more important role than previously thought in shaping regional climate through absorption in and near dust source regions, where most of coarse particles reside.

6.2.2. Chemical mixing states

Aerosol chemical mixing states are defined by the distribution of multiple chemical species across a population of particles within an aerosol. Two mixing states are defined: internal and external. An aerosol of internal mixing means “all particles in the population contain the same species in the same mass fractions”, while an aerosol of external mixing means “every particle contains just one species”, as illustrated in Fig. 16 (Riemer et al., 2019).

Aerosol optical properties, such as scattering and absorption, are partially determined by their mixing states. Generally, the internal mixing can result in a more absorbing aerosol mixture than does external mixing. This is because in internal mixing, the absorbing particles are contained in every mixed aerosol and thus cause all mixed aerosols to become absorbing, which generally exceed that if all the absorbing particles concentrate exclusively on absorbing aerosols (Seinfeld and Pandis, 2016). For example, the global mean of all-sky direct radiative effect of black carbon estimated by core-shell internal mixing can be significantly larger than that estimated by external mixing (Kim et al., 2008; Tuccella et al., 2020).

Activation of fine aerosol particles (diameter $< \sim 1$ μm) is also largely influenced by the mixing state. Generally, dust aerosols are dominated by coarse particles (diameter $> \sim 1$ μm) by mass and surface area size distribution, but they are dominated by fine particles by number size distribution (Mahowald et al., 2014), particularly after a

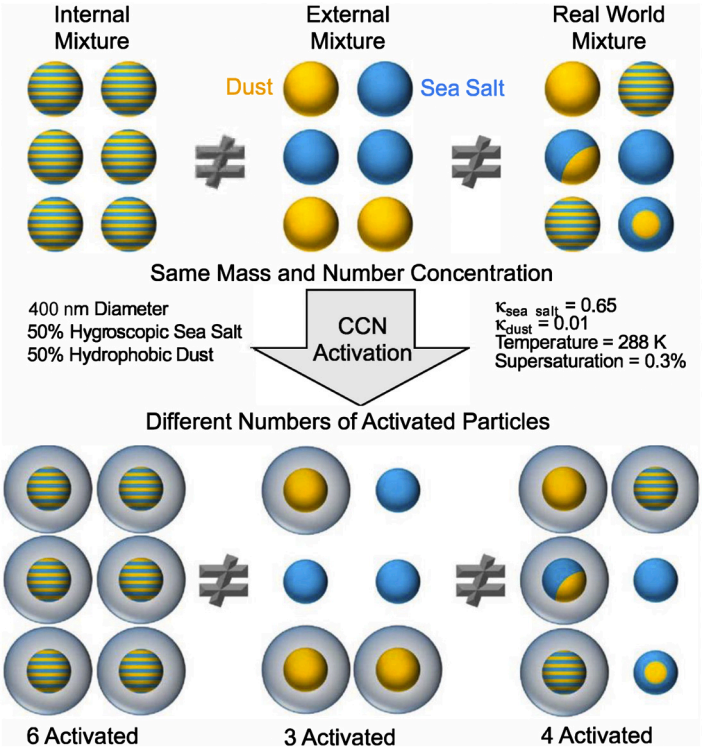


Fig. 16. Illustrative example of how various assumptions about the aerosol mixing states can affect the efficiency of activation of aerosols as cloud condensation nuclei (CCN). For each of mixing state, the six particles together consist of 50% hygroscopic sea salt (blue) and 50% hydrophobic dust (gold) by volume. Particles with blue and yellow stripes comprise the two components of the same volume that are homogeneously distributed within the particle. For this example, a hypothetical particle diameter of 400 nm (i.e., fine dust and sea salt) makes that the chemical composition instead of particle sizes dominate CCN activity. The top populations show the mixing states, while the bottom three populations show particles that would be activate act as CCN at 288 K and 0.3% supersaturation, assuming that sea salt has a hygroscopicity parameter $\kappa = 0.65$ and dust has $\kappa = 0.01$ (modified from Riemer et al. (2019)). (For interpretation of the references to color in this figure legend, the reader is referred to the web version of this article.)

long-distance transport from the source regions (Maring, 2003; Denjean et al., 2016a; Denjean et al., 2016b). Therefore, fine dust aerosols could work as important cloud condensation nuclei (CCN) if they are mixed with hygroscopic aerosol constituents, such as sulfate or sea salt. Fig. 16 is an illustrative example of how the mixing states of dust and sea salt could influence activation of mixed dust. Similar to the reasoning of the absorbing property of mixed dust, internal mixing of dust with sea salt can result in two folds as much activated aerosols as external mixing (Fig. 16). Consequently, the strength of the fine dust and warm cloud interaction can be significantly influenced by assumptions of dust mixing state in the model. Note that the activation of coarse dust particles as ice cloud (Prenni et al., 2009; Tobo et al., 2019; Zhao et al., 2019) is largely determined by particle size (Reicher et al., 2019) and much less dependent on dust hygroscopicity or mixing state than do fine dust particles as CCN in observations.

A real-world aerosol mixing state is between internal and external mixing states. A useful metric to quantify the mixing state is the mixing state index χ (Riemer and West, 2013), which ranges from 0% (a completely externally mixed population) to 100% (a completely internally population). Typical values of χ are 72% when continental pollution dominated and 37% when maritime air mass was prevalent (Healy et al., 2014). Although aerosol mixing state has a large variation indicated by the range of χ and play an important role in calculating aerosol optical properties, in most of current climate models, it is oversimplified, i.e., the aerosols are assumed either fully internally or externally mixed (e.g., Liu et al., 2012; Lee et al., 2016). Therefore, in future development of aerosol schemes, χ should be taken into account to improve the simulation of absorption and activation as CCN of mixed dust aerosols and thus the dust-induced aerosol–radiation (Matsui et al., 2018) and aerosol–cloud (Riemer et al., 2019) interactions. This is particularly important in regions with major aerosol species from difference sources, such as dust and sea salt mixture over the Arabian Sea (Tandule et al., 2020) and the tropical Atlantic Ocean (Prospero and Mayol-Bracero, 2013), biomass burning generated black carbon and sea salt mixture over South Atlantic Ocean (Schill et al., 2020), and carbonaceous–sulfate–nitrate aerosol mixture over urban areas (Snider et al., 2016). For example, dust aerosols emitted from Northwest China can be transported long-distance to urban regions in Southeast China where they can readily get mixed with anthropogenic aerosol species and consequently the mixed dust aerosols are 50% more absorbing than pure dust or anthropogenic aerosols (Tian et al., 2018).

6.2.3. Refractive index

One of the largest uncertainties in simulations of dust optical properties is its complex refractive index, which is expressed as follows,

$$\overline{n} = n + i\kappa, \tag{1}$$

where the real part n is phase velocity accounting for scattering or refraction, while the imaginary part κ is called the extinction coefficient or the mass attenuation coefficient and is responsible for absorption. The influence of κ on radiation absorption can be easily shown in a plane wave. For the electric field of a plane electromagnetic wave traveling in the z-direction, the plane wave can be expressed as:

$$\mathbf{E}(z,t) = e^{-2\pi\kappa z/\lambda_0}\, Re\left[\mathbf{E}_0 e^{i(kz-\omega t)}\right], \tag{2}$$

where $\mathbf{E}_0$ is a constant vector; $k = 2\pi n/\lambda_0$ with λ_0 being the wavelength in the vacuum; ω is the angular frequency and t is time. The density of the electric field is proportional to its square, so the density of light decays by a factor of $e^{4\pi\kappa/\lambda_0}$ as the light travels within a dust particle by a unit distance. Therefore, the absorption of radiation by dust particles increases exponentially with κ but decreases with wavelength.

Both n and κ depend on chemical composition or mineral components of dust aerosols. Hematite and goethite are two iron minerals in dust particles that determine the absorptive properties of dust aerosols (Balkanski et al., 2007; Di Biagio et al., 2019a). Hematite has extremely strong absorption of shortwave radiation, with a larger κ of about 0.9 than elemental carbon ($\kappa = 0.5$) and organic carbon ($\kappa = 0.05$) at 440 nm (Koven and Fung, 2006). Due to different content of iron oxides in dust aerosols emitted from different source regions (Moosmüller et al., 2012), the imaginary part κ varies by almost two orders of magnitude (0.0001 to 0.008 at 550 nm) with the corresponding single scattering albedo (SSA) ranging from 0.99 to 0.80 at 550 nm (Di Biagio et al., 2019a and therein). On the contrast, the real part n of dust refractive index ranges between 1.47 and 1.56 at 550 nm.

The large variations of κ could affect the magnitude and sign of dust directive radiative effect (cooling vs. heating) at TOA on both regional and global scale (Liao and Seinfeld, 1998; Balkanski et al., 2007; Colarco et al., 2014; Tuccella et al., 2020), and change the impact of dust aerosols on regional and global climate (Das et al., 2015; Bangalath and Stenchikov, 2016; Jin et al., 2016a; Strong et al., 2018; Evans et al., 2020). For instance, the global-averaged dust TOA radiative effect at all-sky conditions can vary from -0.21 to $+0.17$ W m^{-2} as κ increases from about 0.004 to 0.008 at 550 nm (Balkanski et al., 2007). Moreover, the debate on the "EHP" hypothesis—inconsistent responses of the Indian summer monsoon rainfall to Asian dust aerosols in models (Nigam and Bollasina, 2011 and therein), could be stemmed from different κ values used in various climate models. For example, increasing κ from zero to 0.008 at 600 nm could cause the response of the ISM rainfall to the Middle East dust aerosols shift from negative (less rainfall) to positive (more rainfall), as shown in Fig. 12 (Jin et al., 2016a).

Despite the large variations of κ and the consequent uncertainties in modeling dust radiative effect and dust–climate interactions, almost all climate models apply a globally constant κ value (Sand et al., 2021), assuming a globally homogeneous content of iron oxides of dust aerosols. However, various studies have shown that iron and iron oxides dust content is highly variable at regional even local scales (Lafon et al., 2006; Di Biagio et al., 2019a). To account for the spatial heterogeneity of dust mineral compositions, global map of dust mineral composition has be derived (Perlwitz et al., 2015a) and incorporated into climate models to simulate dust as component minerals (Perlwitz et al., 2015b; Scanza et al., 2015; Li et al., 2020).

However, the available map of dust mineral composition is derived based on the relation between soil type and mineral composition (Claquin et al., 1999), which is further derived from a very limited number of observations particularly in arid regions that contain dust sources (Perlwitz et al., 2015a). Therefore, a detailed and high-spatial resolution global map of dust mineral composition is required to better resolve the large spatial heterogeneity of dust absorption. To begin in 2022, the Earth surface Mineral dust source InvesTigation (EMIT), a NASA's fourth Earth Venture Instrument project, will map the soil minerology in arid dust source regions around the world (Green et al., 2020). EMIT will use a sensor mounted to the International Space Station to image spectroscopy in the visible and infrared wavelength. A global map of soil minerology with high spatial resolution will be retrieved through these observations. The EMIT products have great potential to improve the simulation of global dust absorption, which will further significantly reduce the uncertainties in estimation of global dust direct radiative effect and dust–climate interactions.

6.3. Anthropogenic dust sources

The term of "dust", so far, has been referred to as the natural dust aerosols, which are emitted from bare surfaces such as deserts. Its counterpart, anthropogenic dust, accounts for a significant fraction of the global total dust emissions (e.g., Webb and Pierre, 2018). However, most climate models do not take into account of anthropogenic dust (Chen et al., 2018), which could cause an underestimation of anthropogenic climate change.

Anthropogenic dust is categorized into direct and indirect emissions based on the way it is emitted (Zender et al., 2004). Direct anthropogenic dust is produced or emitted by human activities, examples of

which include agricultural cultivation, vehicle-based dust emissions from paved and unpaved roads, mining, construction, and so on; while indirect anthropogenic dust represents changes in dust emissions due to human-induced climate change. The contribution of anthropogenic dust, including both categories, to the total dust emissions at the global scale has a large uncertainty, ranging from 10% to 60% (Mahowald and Luo, 2003; Zender et al., 2004). Recent studies constrained this contribution to about 25% using long-term satellite retrievals (Ginoux et al., 2012; Huang et al., 2015).

Although anthropogenic dust plays an important role in global dust cycle, currently, most climate models do not take into account anthropogenic dust sources. The global distribution of dust sources is represented as dust source function or soil erodibility in climate models, which is a measure of the susceptibility of soil particles to detachment from the surface and ejection into the air by strong winds. Various methods were proposed to calculate dust source function, including topographic, geomorphic, and hydrologic methods (Ginoux et al., 2001; Zender, 2003; Grini et al., 2005) as well as satellite-retrieved frequency of absorbing aerosol events (Prospero et al., 2002). These dust source maps were derived to simulate natural dust emissions and thus ignored anthropogenic dust.

New dust source maps should be produced to include anthropogenic dust sources in future simulation of dust cycle. Vegetation indices, such as Normalized Difference Vegetation Index (NDVI), were used to calculate dynamic surface bareness maps that were used as dust source function or soil erodibility in dust emission parameterization scheme (Kim et al., 2013; Xi and Sokolik, 2015). Such a dust source function map may include a portion of anthropogenic dust source regions, such as cropland and pastureland, depending on the chosen threshold of NDVI. Using these dynamic dust source maps, a number of studies estimated the global anthropogenic dust emissions (Chen et al., 2018; Chen et al., 2019) and assessed the improvement of the new dust emission schemes in reproducing dust emissions over the human disturbed vegetated surfaces (Vukovic et al., 2014; Kim et al., 2017).

Due to climate change and human activities, some lakes around the world has been dried up and important new anthropogenic dust sources have been formed (Jin et al., 2017; Parajuli and Zender, 2018), especially in the Middle East and Central Asia (Pekel et al., 2016). For example, the Aral Sea in Central Asia has been dramatically shrinking during the past 4 to 5 decades (Gaybullaev et al., 2012), causing a large part of the lake bottom be exposed to the air and thus more frequent dust storm events (Jin et al., 2017; Li and Sokolik, 2018). However, these newly formed anthropogenic dust sources have not been included in the current dust source maps. The lack of these new anthropogenic dust sources in current research efforts has a clear impact on the estimation of global dust emissions and its trend in future, given that dryland is projected to expand in an accelerated rate during the rest of this century (Feng and Fu, 2013; Huang et al., 2016).

7. Conclusion

In this review, we have identified several physical mechanisms behind the interactions of Asian mineral dust aerosols with the Indian summer monsoon rainfall, and the broad scale ASM, and also addressed the current challenges in numerical simulations of dust physical and chemical properties and the associated climatic impacts at the global scale.

The Asian dust–ISM monsoon interactions involve complex interactions of dust, clouds, circulation, convection and precipitation, as summarized in Fig. 17. Dust aerosols accumulated over the Arabian Sea during the monsoon season are transported from four sources: the Arabian Peninsula, Iran–Afghanistan–Pakistan, the Thar Desert, and the Horn of Africa. These transported dust aerosols can be readily lifted to a high altitude and get stacked over the Arabian Sea along the intertropical discontinuity areas (i.e., with near-zero meridional wind), which is formed by the concurrent of northwesterly Shamal wind and northerly Levar wind from land mass and southwesterly monsoon flow from ocean. Radiative heating through the stacked effect of dust aerosols could induce diabatic heating–dynamical feedback analogous to the EHP (Lau et al., 2006). This results in a strengthening of the northwest

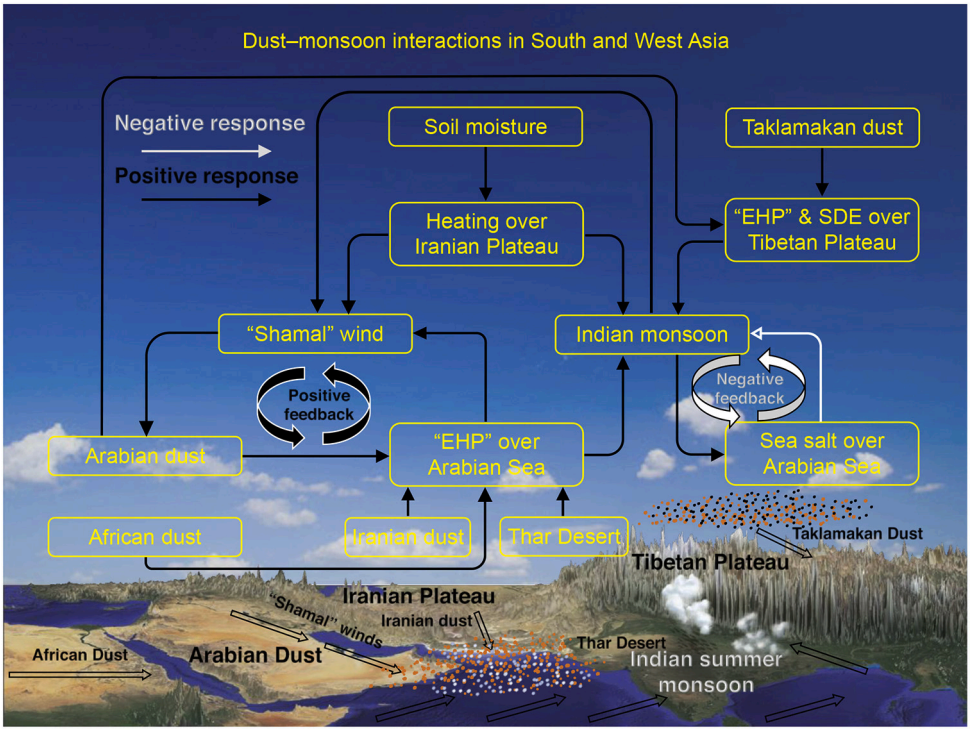


Fig. 17. Schematic diagram showing the interactions between the Asian dust and the ISM monsoon. Dust–ice cloud interaction is discussed in Section 3.4 and not included in this schematic. Acronyms: EHP=Elevated Heat Pump; SDE=Snow Darkening Effect.

Shamal wind and an enhancement of the southwest monsoonal flow. A stronger Shamal wind can cause more dust emissions, forming a positive feedback loop between dust induced EHP effect over the Arabian Sea and the Shamal wind (Jin et al., 2015). On the other hand, the strengthened southwest monsoonal flow can generate more sea salt aerosols (Li and Ramanathan, 2002), which can exert a negative impact on the monsoonal circulations and rainfall through scattering solar radiation and thus cooling the mid-troposphere (Vinoj et al., 2014), which in turn reduces sea salt emissions. As a result, a negative feedback loop exists between the southwest monsoonal flow and sea salt over the Arabian Sea. The observed positive correlation between the monsoonal rainfall and AOD over the Arabian Sea indicates that the positive feedback loop between Shamal wind and the dust induced EHP effect dominates the negative feedback loop between the southwest monsoonal flow and sea salt emissions. Snow-darkening effect (SDE) caused by the deposition of black carbon and dust in snow and ice in the high terrains of the Iranian Plateau and the western Tibetan Plateau during boreal spring and early summer can also reduce the snow albedo and warm the land surface and subsequently the troposphere (Lau and Kim, 2018; Rahimi et al., 2019). A warmer troposphere due to SDE over the Tibetan Plateau can further amplify the EHP effect and modulate the rainfall patterns of the ISM and EASM, through displacement of the jet stream, and development of upper-level wave-train teleconnections.

Additionally, topographic heating over the Iranian Plateau could further strengthens the summer Shamal wind and thus enhance dust emissions and dust transport to the Arabian Sea. This heating has been long recognized as one of the drivers for the initialization and development of the ISM system (Wu et al., 2012; Wu et al., 2017; Zhang et al., 2019b). Dust accumulation over the southern foothills of the Iranian Plateau and West Himalayas can also be effective in inducing EHP dynamical feedback (Lau et al., 2020). Therefore, both dust emissions in the Arabian Peninsula and the monsoonal rainfall could be enhanced by a stronger heating over the Iranian Plateau, which could be an important physical mechanism responsible for the observed positive correlation between AOD over the Arabian Sea and monsoonal rainfall.

The aforementioned physical mechanisms are subject to large uncertainties in observations and model physics. These include dust variability at various timescales (e.g., from interannual to decadal to interdecadal timescales), number size distribution, chemical mixing state, refractive index, and anthropogenic dust sources from agricultural and land use changes (Ginoux et al., 2012; Evan et al., 2014; Jin et al., 2016a; Kok et al., 2017; Di Biagio et al., 2019b). These factors could ultimately affect desert dust–monsoon interaction for the ISM, and regions beyond. More observational and modeling efforts should be devoted to a better understanding of these physical processes and improving their representations in climate models to reduce the uncertainties in dust–monsoon interactions in future.

As a final note, based on studies on impacts of dust aerosols on regional weather and climate in ASM regions revealed by this review, it is likely that dust aerosols could play even more important roles in aerosol–climate interactions than previously believed. As anthropogenic emissions of aerosols and aerosol precursors have been decreasing in Europe (e.g., Provencal et al., 2017), North America (e.g., Jin and Pryor, 2020), and China (e.g., Zhai et al., 2019; Zhang et al., 2019a), and are projected to decrease in India due to clean air actions (Sundaray and Bhardwaj, 2019), natural dust aerosols will account for a larger fraction in total aerosol masses and thus could dominate the aerosol–climate interactions, particularly in Asia due to rapid decrease in anthropogenic aerosol emissions. Moreover, the Northern Hemisphere monsoon system is projected to shift westward due to a westward shift of the North Pacific Subtropical High and South Asia monsoon trough (Hsu et al., 2013; Preethi et al., 2017) and an increase in monsoonal rainfall at the end of this century (Hsu et al., 2013; Lee and Wang, 2014); dryland is also projected to increase significantly (Huang et al., 2016), implying higher dust emissions. Therefore, how dust–monsoon interactions will evolve in the future, and how they can affect the projected changes in both monsoon and dust emissions pose important and challenging questions for further studies.

Declaration of Competing Interest

The authors declare no conflict of financial interests.

Acknowledgments

CW thanks the support provided by L'Agence National de la Recherche (ANR) of France under the "Programme d'Investissements d'Avenir" (ANR-18-MPGA-003 EUROACE). JW is supported by National Science Foundation of China under grants 41975084 and 42088101. Partial support for coauthor WL was provided by the U.S. Department of Energy (DOE), Office of Science, Biological and Environmental Research as part of the Regional and Global Modeling and Analysis Program under Grant Award #300426-00001 to U. of Maryland from the Pacific Northwest NationalLaboratory (PNNL). PNNL is operated for DOE, by Battelle Memorial Institute under contract DE-AC05-76RL01830.

References

Adebiyi, A.A., Kok, J.F., 2020. Climate models miss most of the coarse dust in the atmosphere. Sci. Adv. 6.
Alizadeh Choobari, O., Zawar-Reza, P., Sturman, A., 2012. Feedback between windblown dust and planetary boundary-layer characteristics: Sensitivity to boundary and surface layer parameterizations. Atmos. Environ. 61, 294–304.
Andreae, M.O., Rosenfeld, D., Artaxo, P., Costa, A., Frank, G., Longo, K., Silva-Dias, M.d., 2004. Smoking rain clouds over the Amazon. Science 303, 1337–1342.
Anisimov, A., Axisa, D., Kucera, P.A., Mostamandi, S., Stenchikov, G., 2018. Observations and cloud-resolving modeling of haboob dust storms over the Arabian Peninsula. J. Geophys. Res.-Atmos. 123, 12,147–112,179.
Attada, R., Dasari, H.P., Parekh, A., Chowdary, J.S., Langodan, S., Knio, O., Hoteit, I., 2018. The role of the Indian Summer Monsoon variability on Arabian Peninsula summer climate. Clim. Dyn. 52, 3389–3404.
Badarinath, K.V.S., Kharol, S.K., Kaskaoutis, D.G., Sharma, A.R., Ramaswamy, V., Kambezidis, H.D., 2010. Long-range transport of dust aerosols over the Arabian Sea and Indian region – a case study using satellite data and ground-based measurements. Glob. Planet. Chang. 72, 164–181.
Balkanski, Y., Schulz, M., Claquin, T., Guibert, S., 2007. Reevaluation of Mineral aerosol radiative forcings suggests a better agreement with satellite and AERONET data. Atmos. Chem. Phys. 7, 81–95.
Bangalath, H.K., Stenchikov, G., 2016. Sensitivity of the middle East-North African tropical rainbelt to dust shortwave absorption: a high-resolution AGCM experiment. J. Clim. 29, 7103–7126.
Baustian, K.J., Cziczo, D.J., Wise, M.E., Pratt, K.A., Kulkarni, G., Hallar, A.G., Tolbert, M. A., 2012. Importance of aerosol composition, mixing state, and morphology for heterogeneous ice nucleation: a combined field and laboratory approach. J. Geophys. Res.-Atmos. 117.
Blandford, H.F., 1886. Rainfall of India. In: Monsoon Monograph—India Meteorological Department.
Bollasina, M.A., Ming, Y., Ramaswamy, V., 2011. Anthropogenic aerosols and the weakening of the South Asian summer monsoon. Science 334, 502–505.
Chang, C.-P., Wang, Z., Hendon, H., 2006. The Asian winter monsoon. In: The Asian Monsoon. Springer, pp. 89–127.
Charney, J.G., 1967. The Intertropical Convergence Zone and the Hadley Circulation of the Atmosphere. Department of Meteorology, Massachusetts Institute of Technology.
Chen, J.-P., Hazra, A., Shiu, C.-J., Tsai, I.-C., Lee, H.-H., 2008. Interaction between aerosols and clouds: current understanding. In: Recent Progress in Atmospheric Sciences: Applications to the Asia-Pacific Region. World Scientific, pp. 231–281.
Chen, S., Jiang, N., Huang, J., Xu, X., Zhang, H., Zang, Z., Huang, K., Xu, X., Wei, Y., Guan, X., Zhang, X., Luo, Y., Hu, Z., Feng, T., 2018. Quantifying contributions of natural and anthropogenic dust emission from different climatic regions. Atmos. Environ. 191, 94–104.
Chen, S., Jiang, N., Huang, J., Zang, Z., Guan, X., Ma, X., Luo, Y., Li, J., Zhang, X., Zhang, Y., 2019. Estimations of indirect and direct anthropogenic dust emission at the global scale. Atmos. Environ. 200, 50–60.
Chiang, J.C.H., Friedman, A.R., 2012. Extratropical cooling, interhemispheric thermal gradients, and tropical climate change. Annu. Rev. Earth Planet. Sci. 40, 383–412.
Claquin, T., Schulz, M., Balkanski, Y.J., 1999. Modeling the mineralogy of atmospheric dust sources. J. Geophys. Res.-Atmos. 104, 22243–22256.
Colarco, P.R., Nowottnick, E.P., Randles, C.A., Yi, B.Q., Yang, P., Kim, K.M., Smith, J.A., Bardeen, C.G., 2014. Impact of radiatively interactive dust aerosols in the NASA GEOS-5 climate model: sensitivity to dust particle shape and refractive index. J. Geophys. Res.-Atmos. 119, 753–786.
Creamean, J.M., Suski, K.J., Rosenfeld, D., Cazorla, A., DeMott, P.J., Sullivan, R.C., White, A.B., Ralph, F.M., Minnis, P., Comstock, J.M., 2013. Dust and biological aerosols from the Sahara and Asia influence precipitation in the western US. Science 339, 1572–1578.

Cuevas Agulló, E., 2013. Establishing a WMO Sand and Dust Storm Warning Advisory and Assessment System Regional Node for West Asia: Current Capabilities and Needs: Technical Report.
Cziczo, D.J., Froyd, K.D., Hoose, C., Jensen, E.J., Diao, M., Zondlo, M.A., Smith, J.B., Twohy, C.H., Murphy, D.M., 2013. Clarifying the dominant sources and mechanisms of cirrus cloud formation. Science 340, 1320–1324.
Das, S., Dey, S., Dash, S.K., Giuliani, G., Solmon, F., 2015. Dust aerosol feedback on the Indian summer monsoon: sensitivity to absorption property. J. Geophys. Res.-Atmos. 120, 9642–9652.
Das, S., Giorgi, F., Giuliani, G., 2020. Investigating the relative responses of regional monsoon dynamics to snow darkening and direct radiative effects of dust and carbonaceous aerosols over the Indian subcontinent. Clim. Dyn. 55, 1011–1030.
Dave, P., Bhushan, M., Venkataraman, C., 2017. Aerosols cause intraseasonal short-term suppression of Indian monsoon rainfall. Sci. Rep. 7, 17347.
De, S., Hazra, A., Chaudhari, H.S., 2015. Does the modification in "critical relative humidity" of NCEP CFSv2 dictate Indian mean summer monsoon forecast? Evaluation through thermodynamical and dynamical aspects. Clim. Dyn. 46, 1197–1222.
DeMott, P.J., Sassen, K., Poellot, M.R., Baumgardner, D., Rogers, D.C., Brooks, S.D., Prenni, A.J., Kreidenweis, S.M., 2003. African dust aerosols as atmospheric ice nuclei. Geophys. Res. Lett. 30.
Denjean, C., Cassola, F., Mazzino, A., Triquet, S., Chevaillier, S., Grand, N., Bourrianne, T., Momboisse, G., Sellegri, K., Schwarzenbock, A., Freney, E., Mallet, M., Formenti, P., 2016a. Size distribution and optical properties of mineral dust aerosols transported in the western Mediterranean. Atmos. Chem. Phys. 16, 1081–1104.
Denjean, C., Formenti, P., Desboeufs, K., Chevaillier, S., Triquet, S., Maillé, M., Cazaunau, M., Laurent, B., Mayol-Bracero, O.L., Vallejo, P., Quiñones, M., Gutierrez-Molina, I.E., Cassola, F., Prati, P., Andrews, E., Ogren, J., 2016b. Size distribution and optical properties of African mineral dust after intercontinental transport. J. Geophys. Res.-Atmos. 121, 7117–7138.
D'Errico, M., Cagnazzo, C., Fogli, P.G., Lau, W.K.M., Hardenberg, J., Fierli, F., Cherchi, A., 2015. Indian monsoon and the elevated-heat-pump mechanism in a coupled aerosol-climate model. J. Geophys. Res.-Atmos. 120, 8712–8723.
Di Biagio, C., Formenti, P., Balkanski, Y., Caponi, L., Cazaunau, M., Pangui, E., Journet, E., Nowak, S., Andreae, M.O., Kandler, K., Saeed, T., Piketh, S., Seibert, D., Williams, E., Doussin, J.-F., 2019a. Complex refractive indices and single scattering albedo of global dust aerosols in the shortwave spectrum and relationship to iron content and size. Atmos. Chem. Phys. Discuss. 1–42.
Di Biagio, C., Formenti, P., Balkanski, Y., Caponi, L., Cazaunau, M., Pangui, E., Journet, E., Nowak, S., Andreae, M.O., Kandler, K., Saeed, T., Piketh, S., Seibert, D., Williams, E., Doussin, J.-F., 2019b. Complex refractive indices and single-scattering albedo of global dust aerosols in the shortwave spectrum and relationship to size and iron content. Atmos. Chem. Phys. 19, 15503–15531.
Dimri, A., Yasunari, T., Kotlia, B., Mohanty, U., Sikka, D., 2016. Indian winter monsoon: present and past. Earth Sci. Rev. 163, 297–322.
Duan, A., Hu, J., Xiao, Z., 2013. The Tibetan Plateau summer monsoon in the CMIP5 simulations. J. Clim. 26, 7747–7766.
Evan, A.T., 2018. Surface winds and dust biases in climate models. Geophys. Res. Lett. 45, 1079–1085.
Evan, A.T., Flamant, C., Fiedler, S., Doherty, O., 2014. An analysis of aeolian dust in climate models. Geophys. Res. Lett. 41, 5996–6001.
Evan, A.T., Flamant, C., Gaetani, M., Guichard, F., 2016. The past, present and future of African dust. Nature 531, 493–495.
Evans, S., Dawson, E., Ginoux, P., 2020. Linear relation between shifting ITCZ and dust hemispheric asymmetry. Geophys. Res. Lett. 47 e2020GL090499.
Feng, S., Fu, Q., 2013. Expansion of global drylands under a warming climate. Atmos. Chem. Phys. 13, 10081–10094.
Flanner, M.G., Zender, C.S., Hess, P.G., Mahowald, N.M., Painter, T.H., Ramanathan, V., Rasch, P., 2009. Springtime warming and reduced snow cover from carbonaceous particles. Atmos. Chem. Phys. 9, 2481–2497.
Fountoukis, C., Martín-Pomares, L., Perez-Astudillo, D., Bachour, D., Gladich, I., 2018. Simulating global horizontal irradiance in the Arabian Peninsula: sensitivity to explicit treatment of aerosols. Sol. Energy 163, 347–355.
Francis, D., Alshamsi, N., Cuesta, J., Gokcen Isik, A., Dundar, C., 2019. Cyclogenesis and density currents in the Middle East and the associated dust activity in September 2015. Geosciences 9.
Friedman, A.R., Hwang, Y.-T., Chiang, J.C., Frierson, D.M., 2013. Interhemispheric temperature asymmetry over the twentieth century and in future projections. J. Clim. 26, 5419–5433.
Gadgil, S., 2003. The Indian monsoon and its variability. Annu. Rev. Earth Planet. Sci. 31, 429–467.
Gadgil, S., 2018. The monsoon system: land–sea breeze or the ITCZ? J. Earth Syst. Sci. 127, 1.
Gandham, H., Dasari, H.P., Langodan, S., Karumuri, R.K., Hoteit, I., 2020. Major changes in extreme dust events dynamics over the Arabian Peninsula during 2003–2017 driven by atmospheric conditions. J. Geophys. Res.-Atmos. 125, 1–20 e2020JD032931.
Gautam, R., Hsu, N.C., Lau, W.K.M., Yasunari, T.J., 2013. Satellite observations of desert dust-induced Himalayan snow darkening. Geophys. Res. Lett. 40, 988–993.
Gaybullaev, B., Chen, S.-C., Gaybullaev, D., 2012. Changes in water volume of the Aral Sea after 1960. Appl Water Sci 2, 285–291.
Geen, R., Bordoni, S., Battisti, D.S., Hui, K., 2020. Monsoons, ITCZs, and the concept of the global monsoon. Rev. Geophys. 58 e2020RG000700.
Gerber, H., Frick, G., 2012. Drizzle rates and large sea-salt nuclei in small cumulus. J. Geophys. Res.-Atmos. 117.
Gill, A.E., 1980. Some simple solutions for heat-induced tropical circulation. Q. J. R. Meteorol. Soc. 106, 447–462.
Ginoux, P., Chin, M., Tegen, I., Prospero, J.M., Holben, B., Dubovik, O., Lin, S.J., 2001. Sources and distributions of dust aerosols simulated with the GOCART model. J. Geophys. Res.-Atmos. 106, 20255–20273.
Ginoux, P., Prospero, J.M., Gill, T.E., Hsu, N.C., Zhao, M., 2012. Global-scale attribution of anthropogenic and natural dust sources and their emission rates based on MODIS Deep Blue aerosol products. Rev. Geophys. 50.
Goswami, B., 2005. South Asian monsoon. In: Intraseasonal Variability in the Atmosphere-Ocean Climate System. Springer, pp. 19–61.
Green, R., Mahowald, N., Ung, C., Thompson, D., Bator, L., Bennet, M., Bernas, M., Blackway, N., Bradley, C., Cha, J., Clark, P., Clark, R., Cloud, D., Diaz, E., Dor, E.B., Duren, R., Eastwood, M., Ehlmann, B., Fuentes, L., Ginoux, P., Gross, J., He, Y., Kalashnikova, O., Kert, W., Keymeulen, D., Klimesh, M., Ku, D., Kwong-Fu, H., Liggett, E., Li, L., Lundeen, S., Makowski, M., Mazer, A., Miller, R., Mouroulis, P., Oaida, B., Okin, G., Ortega, A., Oyake, A., Nguyen, H., Pace, T., Painter, T., Pempejian, J., Garcia-Pando, C.P., Pham, T., Phillips, B., Randy, P., Purcell, R., Realmuto, V., Schoolcraft, J., Sen, A., Shin, S., Shaw, L., Soriano, M., Swayze, G., Thingvold, E., Vaid, A., Zan, J., 2020. The Earth surface mineral dust source investigation: an Earth science imaging spectroscopy mission. In: 2020 IEEE Aerospace Conference. IEEE, Big Sky, MT, USA.
Grini, A., Myhre, G., Zender, C.S., Isaksen, I.S., 2005. Model simulations of dust sources and transport in the global atmosphere: effects of soil erodibility and wind speed variability. J. Geophys. Res.-Atmos. 110.
Gu, Y., Xue, Y., De Sales, F., Liou, K.N., 2015. A GCM investigation of dust aerosol impact on the regional climate of North Africa and South/East Asia. Clim. Dyn. 46, 2353–2370.
Halley, E., 1753. An historical account of the trade winds, and monsoons, observable in the seas between and near the Tropicks, with an attempt to assign the physical cause of the said winds. Philos. Trans. R. Soc. Lond. 16, 153–168.
Hari, V., Villarini, G., Karmakar, S., Wilcox, L.J., Collins, M., 2020. Northward propagation of the intertropical convergence zone and strengthening of Indian summer monsoon rainfall. Geophys. Res. Lett. 47.
Hazra, A., Goswami, B.N., Chen, J.-P., 2013a. Role of interactions between aerosol radiative effect, dynamics, and cloud microphysics on transitions of monsoon intraseasonal oscillations. J. Atmos. Sci. 70, 2073–2087.
Hazra, A., Mukhopadhyay, P., Taraphdar, S., Chen, J.P., Cotton, W.R., 2013b. Impact of aerosols on tropical cyclones: an investigation using convection-permitting model simulation. J. Geophys. Res.-Atmos. 118, 7157–7168.
Hazra, A., Chaudhari, H.S., Rao, S.A., Goswami, B.N., Dhakate, A., Pokhrel, S., Saha, S.K., 2015. Impact of revised cloud microphysical scheme in CFSv2 on the simulation of the Indian summer monsoon. Int. J. Climatol. 35, 4738–4755.
Healy, R.M., Riemer, N., Wenger, J.C., Murphy, M., West, M., Poulain, L., Wiedensohler, A., amp, apos, Connor, I.P., McGillicuddy, E., Sodeau, J.R., Evans, G. J., 2014. Single particle diversity and mixing state measurements. Atmos. Chem. Phys. 14, 6289–6299.
Hill, S.A., 2019. Theories for past and future monsoon rainfall changes. Curr. Clim. Change Rep. 5, 160–171.
Hsu, N.C., Gautam, R., Sayer, A.M., Bettenhausen, C., Li, C., Jeong, M.J., Tsay, S.C., Holben, B.N., 2012. Global and regional trends of aerosol optical depth over land and ocean using SeaWiFS measurements from 1997 to 2010. Atmos. Chem. Phys. 12, 8037–8053.
Hsu, P.C., Li, T., Murakami, H., Kitoh, A., 2013. Future change of the global monsoon revealed from 19 CMIP5 models. J. Geophys. Res.-Atmos. 118, 1247–1260.
Hu, Z., Huang, J., Zhao, C., Bi, J., Jin, Q., Qian, Y., Leung, L.R., Feng, T., Chen, S., Ma, J., 2019. Modeling the contributions of Northern Hemisphere dust sources to dust outflow from East Asia. Atmos. Environ. 202, 234–243.
Hu, Z., Huang, J., Zhao, C., Jin, Q., Ma, Y., Yang, B., 2020. Modeling dust sources, transport, and radiative effects at different altitudes over the Tibetan Plateau. Atmos. Chem. Phys. 20, 1507–1529.
Huang, J.P., Liu, J.J., Chen, B., Nasiri, S.L., 2015. Detection of anthropogenic dust using CALIPSO lidar measurements. Atmos. Chem. Phys. 15, 11653–11665.
Huang, J.P., Yu, H.P., Guan, X.D., Wang, G.Y., Guo, R.X., 2016. Accelerated dryland expansion under climate change. Nat. Clim. Chang. 6, 166–171.
Jha, V., Cotton, W.R., Carrió, G.G., Walko, R., 2018. Sensitivity studies on the impact of dust and aerosol pollution acting as cloud nucleating aerosol on orographic precipitation in the Colorado River Basin. Adv. Meteorol. 2018.
Jin, Q., 2015. Intraseasonal Modulation of Indian Summer Monsoon by Middle East Dust: An Observational and Numerical Modeling Study. Doctoral dissertation. The University of Texas at Austin, Austin, Texas, USA.
Jin, Q., Pryor, S.C., 2020. Long-term trends of high aerosol pollution events and their climatic impacts in North America using multiple satellite retrievals and modern-era retrospective analysis for research and applications version 2. J. Geophys. Res.-Atmos. 125, 1–26.
Jin, Q., Wang, C., 2017. A revival of Indian summer monsoon rainfall since 2002. Nat. Clim. Chang. 7, 587–594.
Jin, Q., Wang, C., 2018. The greening of Northwest Indian subcontinent and reduction of dust abundance resulting from Indian summer monsoon revival. Sci. Rep. 8.
Jin, Q., Wei, J., Yang, Z.-L., 2014. Positive response of Indian summer rainfall to Middle East dust. Geophys. Res. Lett. 41, 4068–4074.
Jin, Q., Wei, J., Yang, Z.-L., Pu, B., Huang, J., 2015. Consistent response of Indian summer monsoon to Middle East dust in observations and simulations. Atmos. Chem. Phys. 15, 9897–9915.
Jin, Q., Yang, Z.-L., Wei, J., 2016a. High sensitivity of Indian summer monsoon to Middle East dust absorptive properties. Sci. Rep. 6, 30690.

Jin, Q., Yang, Z.-L., Wei, J., 2016b. Seasonal responses of indian summer monsoon to dust aerosols in the Middle East, India, and China. J. Clim. 29, 632–6349.
Jin, Q., Wei, J., Yang, Z.-L., Lin, P., 2017. Irrigation-induced environmental changes around the aral sea: an integrated view from multiple satellite observations. Remote Sens. 9.
Jin, Q., Wei, J., Pu, B., Yang, Z.L., Parajuli, S.P., 2018. High summertime aerosol loadings over the Arabian Sea and their transport pathways. J. Geophys. Res.-Atmos. 123, 10568–10590.
Kamphus, M., Ettner-Mahl, M., Klimach, T., Drewnick, F., Keller, L., Cziczo, D., Mertes, S., Borrmann, S., Curtius, J., 2010. Chemical composition of ambient aerosol, ice residues and cloud droplet residues in mixed-phase clouds: single particle analysis during the Cloud and Aerosol Characterization Experiment (CLACE 6). Atmos. Chem. Phys. 10, 8077–8095.
Karydis, V.A., Kumar, P., Barahona, D., Sokolik, I.N., Nenes, A., 2011. On the effect of dust particles on global cloud condensation nuclei and cloud droplet number. J. Geophys. Res.-Atmos. 116.
Karydis, V.A., Tsimpidi, A.P., Bacer, S., Pozzer, A., Nenes, A., Lelieveld, J., 2017. Global impact of mineral dust on cloud droplet number concentration. Atmos. Chem. Phys. 17.
Kaskaoutis, D.G., Houssos, E.E., Rashki, A., Francois, P., Legrand, M., Goto, D., Bartzokas, A., Kambezidis, H.D., Takemura, T., 2016. The Caspian Sea–Hindu Kush Index (CasHKI): a regulatory factor for dust activity over southwest Asia. Glob. Planet. Chang. 137, 10–23.
Kaskaoutis, D.G., Houssos, E.E., Solmon, F., Legrand, M., Rashki, A., Dumka, U.C., Francois, P., Gautam, R., Singh, R.P., 2018. Impact of atmospheric circulation types on southwest Asian dust and Indian summer monsoon rainfall. Atmos. Res. 201, 189–205.
KAUST, 2018. Indian summer monsoon keeps Arabian Peninsula hot and dry. In: KAUST Discovery. KAUST. https://discovery.kaust.edu.sa/en/article/631/the-indian-summer-monsoon-keeps-the-arabian-peninsula-hot-and-dry.
Kelly, J.T., Chuang, C.C., Wexler, A.S., 2007. Influence of dust composition on cloud droplet formation. Atmos. Environ. 41, 2904–2916.
Kim, D., Wang, C., Ekman, A.M.L., Barth, M.C., Rasch, P.J., 2008. Distribution and direct radiative forcing of carbonaceous and sulfate aerosols in an interactive size-resolving aerosol–climate model. J. Geophys. Res. 113.
Kim, D., Chin, M., Bian, H., Tan, Q., Brown, M.E., Zheng, T., You, R., Diehl, T., Ginoux, P., Kucsera, T., 2013. The effect of the dynamic surface bareness on dust source function, emission, and distribution. J. Geophys. Res.-Atmos. 118, 871–886.
Kim, M.K., Lau, W.K.M., Kim, K.M., Sang, J., Kim, Y.H., Lee, W.S., 2016. Amplification of ENSO effects on Indian summer monsoon by absorbing aerosols. Clim. Dyn. 46, 2657–2671.
Kim, D., Chin, M., Kemp, E.M., Tao, Z., Peters-Lidard, C.D., Ginoux, P., 2017. Development of high-resolution dynamic dust source function – a case study with a strong dust storm in a regional model. Atmos. Environ. 159, 11–25 (1994).
Kim, M.H., Omar, A.H., Tackett, J.L., Vaughan, M.A., Winker, D.M., Trepte, C.R., Hu, Y., Liu, Z., Poole, L.R., Pitts, M.C., Kar, J., Magill, B.E., 2018. The CALIPSO version 4 automated aerosol classification and lidar ratio selection algorithm. Atmos. Meas. Tech. 11, 6107–6135.
Klingmüller, K., Pozzer, A., Metzger, S., Stenchikov, G.L., Lelieveld, J., 2016. Aerosol optical depth trend over the Middle East. Atmos. Chem. Phys. 16, 5063–5073.
Kok, J.F., 2011. A scaling theory for the size distribution of emitted dust aerosols suggests climate models underestimate the size of the global dust cycle. Proc. Natl. Acad. Sci. U. S. A. 108, 1016–1021.
Kok, J.F., Albani, S., Mahowald, N.M., Ward, D.S., 2014a. An improved dust emission model – Part 2: evaluation in the Community Earth System Model, with implications for the use of dust source functions. Atmos. Chem. Phys. 14, 13043–13061.
Kok, J.F., Mahowald, N.M., Fratini, G., Gillies, J.A., Ishizuka, M., Leys, J.F., Mikami, M., Park, M.S., Park, S.U., Van Pelt, R.S., Zobeck, T.M., 2014b. An improved dust emission model – Part 1: model description and comparison against measurements. Atmos. Chem. Phys. 14, 13023–13041.
Kok, J.F., Ridley, D.A., Zhou, Q., Miller, R.L., Zhao, C., Heald, C.L., Ward, D.S., Albani, S., Haustein, K., 2017. Smaller desert dust cooling effect estimated from analysis of dust size and abundance. Nat. Geosci. 10, 274–278.
Kok, J.F., Ward, D.S., Mahowald, N.M., Evan, A.T., 2018. Global and regional importance of the direct dust-climate feedback. Nat. Commun. 9, 241.
Konwar, M., Maheskumar, R.S., Kulkarni, J.R., Freud, E., Goswami, B.N., Rosenfeld, D., 2012. Aerosol control on depth of warm rain in convective clouds. J. Geophys. Res.-Atmos. 117.
Koven, C.D., Fung, I., 2006. Inferring dust composition from wavelength-dependent absorption in Aerosol Robotic Network (AERONET) data. J. Geophys. Res.-Atmos. 111.
Kovilakam, M., Mahajan, S., 2016. Confronting the “Indian summer monsoon response to black carbon aerosol” with the uncertainty in its radiative forcing and beyond. J. Geophys. Res.-Atmos. 121, 7833–7852.
Kuhlmann, J., Quaas, J., 2010. How can aerosols affect the Asian summer monsoon? Assessment during three consecutive pre-monsoon seasons from CALIPSO satellite data. Atmos. Chem. Phys. 10, 4673–4688.
Kumar, S., Hazra, A., Goswami, B.N., 2013. Role of interaction between dynamics, thermodynamics and cloud microphysics on summer monsoon precipitating clouds over the Myanmar Coast and the Western Ghats. Clim. Dyn. 43, 911–924.
Kumar, A., Suresh, K., Rahaman, W., 2020. Geochemical characterization of modern aeolian dust over the Northeastern Arabian Sea: implication for dust transport in the Arabian Sea. Sci. Total Environ. 729, 138576.
Kumari, B.P., Goswami, B.N., 2010. Seminal role of clouds on solar dimming over the Indian monsoon region. Geophys. Res. Lett. 37.
Lafon, S., Sokolik, I.N., Rajot, J.L., Caquineau, S., Gaudichet, A., 2006. Characterization of iron oxides in mineral dust aerosols: implications for light absorption. J. Geophys. Res.-Atmos. 111.
Lau, W.K.M., 2016. The aerosol-monsoon climate system of Asia: a new paradigm. J. Meteorol. Res. 30, 1–11.
Lau, K.M., Kim, K.M., 2006. Observational relationships between aerosol and Asian monsoon rainfall, and circulation. Geophys. Res. Lett. 33.
Lau, W.K.M., Kim, K.-M., 2010. Fingerprinting the impacts of aerosols on long-term trends of the Indian summer monsoon regional rainfall. Geophys. Res. Lett. 37.
Lau, K.M., Kim, K.M., 2011. Comment on '"Elevated heat pump' hypothesis for the aerosol-monsoon hydroclimate link: 'Grounded' in observations?" by S. Nigam and M. Bollasina. J. Geophys. Res.-Atmos. 116.
Lau, W.K.M., Kim, K.M., 2017. Competing influences of greenhouse warming and aerosols on Asian Summer Monsoon circulation and rainfall. Asia-Pac. J. Atmos. Sci. 53, 181–194.
Lau, W.K.M., Kim, K.M., 2018. Impact of snow-darkening by deposition of light-absorbing aerosols on snow cover in the Himalaya-Tibetan-Plateau and influence on the Asian Summer monsoon: a possible mechanism for the Blanford Hypothesis. Atmosphere (Basel) 9, 438.
Lau, K.M., Kim, M.K., Kim, K.M., 2006. Asian summer monsoon anomalies induced by aerosol direct forcing: the role of the Tibetan Plateau. Clim. Dyn. 26, 855–864.
Lau, K.M., Ramanathan, V., Wu, G.X., Li, Z., Tsay, S.C., Hsu, C., Sikka, R., Holben, B., Lu, D., Tartari, G., Chin, M., Koudelova, P., Chen, H., Ma, Y., Huang, J., Taniguchi, K., Zhang, R., 2008. The joint aerosol–monsoon experiment: a new challenge for monsoon climate research. Bull. Am. Meteorol. Soc. 89, 369–384.
Lau, W.K., Kim, K.-M., Hsu, C.N., Holben, B.N., 2009. Possible influences of air pollution, dust and sandstorms on the Indian monsoon. WMO Bull. 58, 22–30.
Lau, W.K.M., Kim, M.-K., Kim, K.-M., Lee, W.-S., 2010. Enhanced surface warming and accelerated snow melt in the Himalayas and Tibetan Plateau induced by absorbing aerosols. Environ. Res. Lett. 5.
Lau, W.K.M., Kim, K.-M., Shi, J.-J., Matsui, T., Chin, M., Tan, Q., Peters-Lidard, C., Tao, W.K., 2016. Impacts of aerosol–monsoon interaction on rainfall and circulation over Northern India and the Himalaya Foothills. Clim. Dyn. 49, 1945–1960.
Lau, W.K.M., Yuan, C., Li, Z., 2018. Origin, maintenance and variability of the Asian Tropopause Aerosol Layer (ATAL): the roles of monsoon dynamics. Sci. Rep. 8, 3960.
Lau, W.K.M., Kim, K.-M., Zhao, C., Leung, L.R., Park, S.-H., 2020. Impact of dust-cloud-radiation-precipitation dynamical feedback on subseasonal-to-seasonal variability of the asian summer monsoon in global variable-resolution simulations with MPAS-CAM5. Front. Earth Sci. 8.
Lee, J.Y., Wang, B., 2014. Future change of global monsoon in the CMIP5. Clim. Dyn. 42, 101–119.
Lee, S.-Y., Wang, C., 2015. The response of the South Asian summer monsoon to temporal and spatial variations in absorbing aerosol radiative forcing. J. Clim. 28, 6626–6646.
Lee, S.-Y., Shin, H.-J., Wang, C., 2013. Nonlinear effects of coexisting surface and atmospheric forcing of anthropogenic absorbing aerosols: impact on the South Asian monsoon onset. J. Clim. 26, 5594–5607.
Lee, H.-H., Chen, S.-H., Kleeman, M.J., Zhang, H., DeNero, S.P., Joe, D.K., 2016. Implementation of warm-cloud processes in a source-oriented WRF/Chem model to study the effect of aerosol mixing state on fog formation in the Central Valley of California. Atmos. Chem. Phys. 16, 8353–8374.
Lei, H., Wang, J.X.L., 2014. Observed characteristics of dust storm events over the western United States using meteorological, satellite, and air quality measurements. Atmos. Chem. Phys. 14, 7847–7857.
Léon, J.-F., Legrand, M., 2003. Mineral dust sources in the surroundings of the north Indian Ocean. Geophys. Res. Lett. 30.
Levin, Z., Cotton, W.R., 2008. Aerosol Pollution Impact on Precipitation: A Scientific Review. Springer Science & Business Media.
Li, F., Ramanathan, V., 2002. Winter to summer monsoon variation of aerosol optical depth over the tropical Indian Ocean. J. Geophys. Res.-Atmos. 107.
Li, W., Shao, L., 2009. Observation of nitrate coatings on atmospheric mineral dust particles. Atmos. Chem. Phys. 9, 1863–1871.
Li, L.L., Sokolik, I.N., 2018. The dust direct radiative impact and its sensitivity to the land surface state and key minerals in the WRF-Chem-DuMo model: a case study of dust storms in Central Asia. J. Geophys. Res.-Atmos. 123, 4564–4582.
Li, F., Ginoux, P., Ramaswamy, V., 2010. Transport of patagonian dust to Antarctica. J. Geophys. Res. 115.
Li, Z.Q., Lau, W.K.M., Ramanathan, V., Wu, G., Ding, Y., Manoj, M.G., Liu, J., Qian, Y., Li, J., Zhou, T., Fan, J., Rosenfeld, D., Ming, Y., Wang, Y., Huang, J., Wang, B., Xu, X., Lee, S.S., Cribb, M., Zhang, F., Yang, X., Zhao, C., Takemura, T., Wang, K., Xia, X., Yin, Y., Zhang, H., Guo, J., Zhai, P.M., Sugimoto, N., Babu, S.S., Brasseur, G. P., 2016. Aerosol and monsoon climate interactions over Asia. Rev. Geophys. 54, 866–929.
Li, L., Mahowald, N.M., Miller, R.L., Pérez García-Pando, C., Klose, M., Hamilton, D.S., Gonçalves Ageitos, M., Ginoux, P., Balkanski, Y., Green, R.O., 2020. Quantifying the range of the dust direct radiative effect due to source mineralogy uncertainty. Atmos. Chem. Phys. Discuss. 1–58.
Liao, H., Seinfeld, J.H., 1998. Radiative forcing by mineral dust aerosols: sensitivity to key variables. J. Geophys. Res.-Atmos. 103, 31637–31645.
Lin, C., Chen, D.L., Yang, K., Qu, T., 2018. Impact of model resolution on simulating the water vapor transport through the central Himalayas: implication for models' wet bias over the Tibetan Plateau. Clim. Dyn. 51, 3195–3207.
Liu, X., Easter, R.C., Ghan, S.J., Zaveri, R., Rasch, P., Shi, X., Lamarque, J.F., Gettelman, A., Morrison, H., Vitt, F., Conley, A., Park, S., Neale, R., Hannay, C., Ekman, A.M.L., Hess, P., Mahowald, N., Collins, W., Iacono, M.J., Bretherton, C.S., Flanner, M.G., Mitchell, D., 2012. Toward a minimal representation of aerosols in

climate models: description and evaluation in the Community Atmosphere Model CAM5. Geosci. Model Dev. 5, 709–739.
Lohmann, U., Feichter, J., 2005. Global indirect aerosol effects: a review. Atmos. Chem. Phys. 5, 715–737.
Mahowald, N.M., Luo, C., 2003. A less dusty future? Geophys. Res. Lett. 30.
Mahowald, N.M., Kloster, S., Engelstaedter, S., Moore, J.K., Mukhopadhyay, S., McConnell, J.R., Albani, S., Doney, S.C., Bhattacharya, A., Curran, M.A.J., Flanner, M.G., Hoffman, F.M., Lawrence, D.M., Lindsay, K., Mayewski, P.A., Neff, J., Rothenberg, D., Thomas, E., Thornton, P.E., Zender, C.S., 2010. Observed 20th century desert dust variability: impact on climate and biogeochemistry. Atmos. Chem. Phys. 10, 10875–10893.
Mahowald, N., Albani, S., Kok, J.F., Engelstaeder, S., Scanza, R., Ward, D.S., Flanner, M. G., 2014. The size distribution of desert dust aerosols and its impact on the Earth system. Aeolian Res. 15, 53–71.
Maring, H., 2003. Mineral dust aerosol size distribution change during atmospheric transport. J. Geophys. Res. 108.
Matsui, H., Hamilton, D.S., Mahowald, N.M., 2018. Black carbon radiative effects highly sensitive to emitted particle size when resolving mixing-state diversity. Nat. Commun. 9, 3446.
Matsuki, A., Schwarzenboeck, A., Venzac, H., Laj, P., Crumeyrolle, S., Gomes, L., 2010. Cloud processing of mineral dust: direct comparison of cloud residual and clear sky particles during AMMA aircraft campaign in summer 2006. Atmos. Chem. Phys. 10, 1057–1069.
Matsuno, T., 1966. Quasi-geostrophic motions in the equatorial area. J. Meteorol. Soc. Jpn. Ser. II 44, 25–43.
Meehl, G.A., Arblaster, J.M., Collins, W.D., 2008. Effects of black carbon aerosols on the Indian monsoon. J. Clim. 21, 2869–2882.
Miller, R.L., Cakmur, R.V., Perlwitz, J., Geogdzhayev, I.V., Ginoux, P., Koch, D., Kohfeld, K.E., Prigent, C., Ruedy, R., Schmidt, G.A., Tegen, I., 2006. Mineral dust aerosols in the NASA Goddard Institute for Space Sciences ModelE atmospheric general circulation model. J. Geophys. Res. 111.
Moosmüller, H., Engelbrecht, J.P., Skiba, M., Frey, G., Chakrabarty, R.K., Arnott, W.P., 2012. Single scattering albedo of fine mineral dust aerosols controlled by iron concentration. J. Geophys. Res.-Atmos. 117.
Mujumdar, M., Preethi, B., Sabin, T.P., Ashok, K., Saeed, S., Pai, D.S., Krishnan, R., 2012. The Asian summer monsoon response to the La Niña event of 2010. Meteorol. Appl. 19, 216–225.
Murray, B., O'sullivan, D., Atkinson, J., Webb, M., 2012. Ice nucleation by particles immersed in supercooled cloud droplets. Chem. Soc. Rev. 41, 6519–6554.
Nenes, A., Murray, B., Bougiatioti, A., 2014. Mineral dust and its microphysical interactions with clouds. In: Mineral Dust. Springer, pp. 287–325.
Nigam, S., Bollasina, M., 2010. "Elevated heat pump" hypothesis for the aerosol-monsoon hydroclimate link: "Grounded" in observations? J. Geophys. Res.-Atmos. 115.
Nigam, S., Bollasina, M., 2011. Reply to comment by K. M. Lau and K. M. Kim on '"Elevated heat pump' hypothesis for the aerosol-monsoon hydroclimate link: 'Grounded' in observations?". J. Geophys. Res.-Atmos. 116.
Parajuli, S.P., Zender, C.S., 2018. Projected changes in dust emissions and regional air quality due to the shrinking Salton Sea. Aeolian Res. 33, 82–92.
Patel, P.N., Gautam, R., Michibata, T., Gadhavi, H., 2019. Strengthened indian summer monsoon precipitation susceptibility linked to dust-induced ice cloud modification. Geophys. Res. Lett. 46, 8431–8441.
Pekel, J.F., Cottam, A., Gorelick, N., Belward, A.S., 2016. High-resolution mapping of global surface water and its long-term changes. Nature 540, 418–422.
Perlwitz, J.P., Garcia-Pando, C.P., Miller, R.L., 2015a. Predicting the mineral composition of dust aerosols – Part 1: representing key processes. Atmos. Chem. Phys. 15, 11593–11627.
Perlwitz, J.P., Garcia-Pando, C.P., Miller, R.L., 2015b. Predicting the mineral composition of dust aerosols – Part 2: model evaluation and identification of key processes with observations. Atmos. Chem. Phys. 15, 11629–11652.
Pratt, K.A., DeMott, P.J., French, J.R., Wang, Z., Westphal, D.L., Heymsfield, A.J., Twohy, C.H., Prenni, A.J., Prather, K.A., 2009. In situ detection of biological particles in cloud ice-crystals. Nat. Geosci. 2, 398–401.
Preethi, B., Mujumdar, M., Kripalani, R.H., Prabhu, A., Krishnan, R., 2016. Recent trends and tele-connections among South and East Asian summer monsoons in a warming environment. Clim. Dyn. 48, 2489–2505.
Preethi, B., Mujumdar, M., Prabhu, A., Kripalani, R., 2017. Variability and teleconnections of South and East Asian summer monsoons in present and future projections of CMIP5 climate models. Asia-Pac. J. Atmos. Sci. 53, 305–325.
Prenni, A.J., Petters, M.D., Kreidenweis, S.M., Heald, C.L., Martin, S.T., Artaxo, P., Garland, R.M., Wollny, A.G., Pöschl, U., 2009. Relative roles of biogenic emissions and Saharan dust as ice nuclei in the Amazon basin. Nat. Geosci. 2, 402–405.
Prospero, J.M., Mayol-Bracero, O.L., 2013. Understanding the transport and impact of African dust on the Caribbean Basin. Bull. Am. Meteorol. Soc. 94, 1329–1337.
Prospero, J.M., Ginoux, P., Torres, O., Nicholson, S.E., Gill, T.E., 2002. Environmental characterization of global sources of atmospheric soil dust identified with the Nimbus 7 Total Ozone Mapping Spectrometer (TOMS) absorbing aerosol product. Rev. Geophys. 40.
Provencal, S., Kishcha, P., da Silva, A.M., Elhacham, E., Alpert, P., 2017. AOD distributions and trends of major aerosol species over a selection of the world's most populated cities based on the 1st Version of NASA's MERRA Aerosol Reanalysis. Urban Clim. 20, 168–191.
Pu, B., Ginoux, P., 2016. The impact of the Pacific Decadal Oscillation on springtime dust activity in Syria. Atmos. Chem. Phys. 16, 13431–13448.
Pu, B., Ginoux, P., 2017. Projection of American dustiness in the late 21(st) century due to climate change. Sci. Rep. 7.
Pu, B., Ginoux, P., 2018. Climatic factors contributing to long-term variations in surface fine dust concentration in the United States. Atmos. Chem. Phys. 18, 4201–4215.
Pu, B., Ginoux, P., Kapnick, S.B., Yang, X., 2019. Seasonal prediction potential for springtime dustiness in the United States. Geophys. Res. Lett. 46, 9163–9173.
Pu, B., Ginoux, P., Guo, H., Hsu, N.C., Kimball, J., Marticorena, B., Malyshev, S., Naik, V., amp, apos, Neill, N.T., Pérez García-Pando, C., Paireau, J., Prospero, J.M., Shevliakova, E., Zhao, M., 2020. Retrieving the global distribution of the threshold of wind erosion from satellite data and implementing it into the Geophysical Fluid Dynamics Laboratory land–atmosphere model (GFDL AM4.0/LM4.0). Atmos. Chem. Phys. 20, 55–81.
Qian, Y., Yasunari, T.J., Doherty, S.J., Flanner, M.G., Lau, W.K.M., Ming, J., Wang, H., Wang, M., Warren, S.G., Zhang, R., 2014. Light-absorbing particles in snow and ice: measurement and modeling of climatic and hydrological impact. Adv. Atmos. Sci. 32, 64–91.
Rahimi, S., Liu, X., Wu, C., Lau, W.K., Brown, H., Wu, M., Qian, Y., 2019. Quantifying snow darkening and atmospheric radiative effects of black carbon and dust on the South Asian monsoon and hydrological cycle: experiments using variable-resolution CESM. Atmos. Chem. Phys. 19, 12025–12049.
Rahul, P.R.C., Salvekar, P.S., Devara, P.C.S., 2008. Aerosol optical depth variability over Arabian Sea during drought and normal years of Indian monsoon. Geophys. Res. Lett. 35.
Rajeevan, M., Gadgil, S., Bhate, J., 2010. Active and break spells of the Indian summer monsoon. J. Earth Syst. Sci. 119, 229–247.
Ramage, C.S., 1971. Monsoon meteorology. In: International geophysics series. Academic Press.
Ramanathan, V., Chung, C., Kim, D., Bettge, T., Buja, L., Kiehl, J.T., Washington, W.M., Fu, Q., Sikka, D.R., Wild, M., 2005. Atmospheric brown clouds: impacts on South Asian climate and hydrological cycle. Proc. Natl. Acad. Sci. U. S. A. 102, 5326–5333.
Ramaswamy, V., Muraleedharan, P.M., Babu, C.P., 2017. Mid-troposphere transport of Middle-East dust over the Arabian Sea and its effect on rainwater composition and sensitive ecosystems over India. Sci. Rep. 7, 13676.
Randel, W.J., Park, M., Emmons, L., Kinnison, D., Bernath, P., Walker, K.A., Boone, C., Pumphrey, H., 2010. Asian monsoon transport of pollution to the stratosphere. Science 328, 611–613.
Rao, Y., 1976. Southwest Monsoon. Meteorological Monograph, Synoptic Meteorology, Vols. 366, 379. India Meteorological Department, New Delhi.
Rashki, A., Kaskaoutis, D.G., Mofidi, A., Minvielle, F., Chiapello, I., Legrand, M., Dumka, U.C., Francois, P., 2019. Effects of Monsoon, Shamal and Levar winds on dust accumulation over the Arabian Sea during summer – The July 2016 case. Aeolian Res. 36, 27–44.
Ratnam, M.V., Santhi, Y.D., Kishore, P., Rao, S.V.B., 2014. Solar cycle effects on Indian summer monsoon dynamics. J. Atmos. Sol. Terr. Phys. 121, 145–156.
Reicher, N., Budke, C., Eickhoff, L., Raveh-Rubin, S., Kaplan-Ashiri, I., Koop, T., Rudich, Y., 2019. Size-dependent ice nucleation by airborne particles during dust events in the eastern Mediterranean. Atmos. Chem. Phys. 19, 11143–11158.
Riehl, H., 1954. Tropical Meteorology (p. 392). McGraw Hill, New York.
Riehl, H., 1979. Climate and Weather in the Tropics. Academic Press.
Riemer, N., West, M., 2013. Quantifying aerosol mixing state with entropy and diversity measures. Atmos. Chem. Phys. 13, 11423–11439.
Riemer, N., Ault, A.P., West, M., Craig, R.L., Curtis, J.H., 2019. Aerosol mixing state: measurements, modeling, and impacts. Rev. Geophys. 57, 187–249.
Rodwell, M.J., Hoskins, B.J., 1996. Monsoons and the dynamics of deserts. Q. J. R. Meteorol. Soc. 122, 1385–1404.
Rodwell, M.J., Hoskins, B.J., 2001. Subtropical anticyclones and summer monsoons. J. Clim. 14, 3192–3211.
Rosenfeld, D., 2006. Aerosols, clouds, and climate. Science 312, 1323–1324.
Rosenfeld, D., Rudich, Y., Lahav, R., 2001. Desert dust suppressing precipitation: a possible desertification feedback loop. In: Proceedings of the National Academy of Sciences, Vol. 98, pp. 5975–5980.
Rosenfeld, D., Lohmann, U., Raga, G.B., O'Dowd, C.D., Kulmala, M., Fuzzi, S., Reissell, A., Andreae, M.O., 2008. Flood or drought: how do aerosols affect precipitation? Science 321, 1309–1313.
Roxy, M.K., Ritika, K., Terray, P., Murtugudde, R., Ashok, K., Goswami, B.N., 2015. Drying of Indian subcontinent by rapid Indian Ocean warming and a weakening land-sea thermal gradient. Nat. Commun. 6.
Saha, S.K., Hazra, A., Pokhrel, S., Chaudhari, H.S., Sujith, K., Rai, A., Rahaman, H., Goswami, B.N., 2019. Unraveling the mystery of indian summer monsoon prediction: improved estimate of predictability limit. J. Geophys. Res.-Atmos. 4, 1962–1974.
Saha, S.K., Hazra, A., Pokhrel, S., Chaudhari, H.S., Rai, A., Sujith, K., Rahaman, H., Goswami, B., 2020. Reply to Comment by ET Swenson, D. Das, and J. Shukla on "Unraveling the mystery of indian summer monsoon prediction: improved estimate of predictability limit". J. Geophys. Res.-Atmos. 125 e2020JD033242.
Sanap, S.D., Pandithurai, G., 2015. The effect of absorbing aerosols on Indian monsoon circulation and rainfall: a review. Atmos. Res. 164-165, 318–327.
Sand, M., Samset, B.H., Myhre, G., Gliß, J., Bauer, S.E., Bian, H., Chin, M., Checa-Garcia, R., Ginoux, P., Kipling, Z., Kirkevåg, A., Kokkola, H., Sager, P.L., Tund, M.T., Matsui, H., van Noije, T., Remy, S., Schulz, M., Stier, P., Stjern, C.W., Takemura, T., Tsigaridis, K., Tsyro, S.G., Watson-Parris, D., 2021. Aerosol absorption in global models from AeroCom Phase III. Atmospheric Chemistry and Physics Discussions 1–36.
Sarangi, C., Qian, Y., Rittger, K., Ruby Leung, L., Chand, D., Bormann, K.J., Painter, T.H., 2020. Dust dominates high-altitude snow darkening and melt over high-mountain Asia. Nat. Clim. Chang. 10, 1045–1051.
Scanza, R.A., Mahowald, N., Ghan, S., Zender, C.S., Kok, J.F., Liu, X., Zhang, Y., Albani, S., 2015. Modeling dust as component minerals in the Community

Atmosphere Model: development of framework and impact on radiative forcing. Atmos. Chem. Phys. 15, 537–561.
Schill, G.P., Froyd, K.D., Bian, H., Kupc, A., Williamson, C., Brock, C.A., Ray, E., Hornbrook, R.S., Hills, A.J., Apel, E.C., Chin, M., Colarco, P.R., Murphy, D.M., 2020. Widespread biomass burning smoke throughout the remote troposphere. Nat. Geosci. 13, 422–427.
Seinfeld, J.H., Pandis, S.N., 2016. Atmospheric Chemistry and Physics: From Air Pollution to Climate Change. John Wiley & Sons.
Shao, Y., Klose, M., Wyrwoll, K.-H., 2013. Recent global dust trend and connections to climate forcing. J. Geophys. Res.-Atmos. 118, 11,107–111,118.
Sharma, D., Miller, R.L., 2017. Revisiting the observed correlation between weekly averaged Indian monsoon precipitation and Arabian Sea aerosol optical depth. Geophys. Res. Lett. 44, 10006–10016.
Shi, Z., Xie, X., Li, X., Yang, L., Xie, X., Lei, J., Sha, Y., Liu, X., 2019. Snow-darkening versus direct radiative effects of mineral dust aerosol on the Indian summer monsoon onset: role of temperature change over dust sources. Atmos. Chem. Phys. 19, 1605–1622.
Sikka, D., Gadgil, S., 1980. On the maximum cloud zone and the ITCZ over Indian, longitudes during the southwest monsoon. Mon. Weather Rev. 108, 1840–1853.
Simpson, G., 1921. The south-west monsoon. Q. J. R. Meteorol. Soc. 47, 151–171.
Singh, A.P., Mohanty, U.C., Sinha, P., Mandal, M., 2007. Influence of different land-surface processes on Indian summer monsoon circulation. Nat. Hazards 42, 423–438.
Singh, C., Thomas, L., Kumar, K.K., 2015. Impact of aerosols and cloud parameters on Indian summer monsoon rain at intraseasonal scale: a diagnostic study. Theor. Appl. Climatol. 127, 381–392.
Singh, C., Ganguly, D., Sharma, P., 2019. Impact of West Asia, Tibetan Plateau and local dust emissions on intra-seasonal oscillations of the South Asian monsoon rainfall. Clim. Dyn. 53, 6569–6593.
Smith, M.B., Mahowald, N.M., Albani, S., Perry, A., Losno, R., Qu, Z., Marticorena, B., Ridley, D.A., Heald, C.L., 2017. Sensitivity of the interannual variability of mineral aerosol simulations to meteorological forcing dataset. Atmos. Chem. Phys. 17, 3253–3278.
Snider, G., Weagle, C.L., Murdymootoo, K.K., Ring, A., Ritchie, Y., Stone, E., Walsh, A., Akoshile, C., Anh, N.X., Balasubramanian, R., Brook, J., Qonitan, F.D., Dong, J., Griffith, D., He, K., Holben, B.N., Kahn, R., Lagrosas, N., Lestari, P., Ma, Z., Misra, A., Norford, L.K., Quel, E.J., Salam, A., Schichtel, B., Segev, L., Tripathi, S., Wang, C., Yu, C., Zhang, Q., Zhang, Y., Brauer, M., Cohen, A., Gibson, M.D., Liu, Y., Martins, J. V., Rudich, Y., Martin, R.V., 2016. Variation in global chemical composition of PM2.5: emerging results from SPARTAN. Atmos. Chem. Phys. 16, 9629–9653.
Sokolik, I.N., Winker, D., Bergametti, G., Gillette, D., Carmichael, G., Kaufman, Y., Gomes, L., Schuetz, L., Penner, J., 2001. Introduction to special section: outstanding problems in quantifying the radiative impacts of mineral dust. J. Geophys. Res.-Atmos. 106, 18015–18027.
Solmon, F., Nair, V.S., Mallet, M., 2015. Increasing Arabian dust activity and the Indian summer monsoon. Atmos. Chem. Phys. 15, 8051–8064.
Stanhill, G., Cohen, S., 2001. Global dimming: a review of the evidence for a widespread and significant reduction in global radiation with discussion of its probable causes and possible agricultural consequences. Agric. For. Meteorol. 107, 255–278.
Strong, J.D.O., Vecchi, G.A., Ginoux, P., 2018. The climatological effect of saharan dust on global tropical cyclones in a fully coupled GCM. J. Geophys. Res.-Atmos. 123, 5538–5559.
Stuut, J.-B., Prins, M.A., 2014. The significance of particle size of long-range transported mineral dust. Past Glob. Changes Mag. 22, 14–15.
Sullivan, R., Moore, M., Petters, M., Kreidenweis, S., Roberts, G., Prather, K., 2009. Effect of chemical mixing state on the hygroscopicity and cloud nucleation properties of calcium mineral dust particles. Atmos. Chem. Phys. 9.
Sundaray, S.N.K., Bhardwaj, S.R., 2019. National Clean Air Programme. Indian Ministry of Environment, Forest & Climate Change, pp. 1–122.
Swenson, E.T., Das, D., Shukla, J., 2020. Comment on “Unraveling the mystery of Indian summer monsoon prediction: improved estimate of predictability limit” by Saha et al. J. Geophys. Res.-Atmos. 125 e2020JD033037.
Tandule, C.R., Kalluri, R.O.R., Gugamsetty, B., Kotalo, R.G., Thotli, L.R., Rajuru, R.R., Vaddin, S., 2020. Decadal climatology of the spatial and vertical distributions of tropospheric aerosol over the Arabian Sea based on satellite observations. Int. J. Climatol. 40, 4676–4689.
Tang, Y., Han, Y., Ma, X., Liu, Z., 2018. Elevated heat pump effects of dust aerosol over Northwestern China during summer. Atmos. Res. 203, 95–104.
Tegen, I., Lacis, A.A., 1996. Modeling of particle size distribution and its influence on the radiative properties of mineral dust aerosol. J. Geophys. Res.-Atmos. 101, 19237–19244.
Tian, P., Zhang, L., Ma, J., Tang, K., Xu, L., Wang, Y., Cao, X., Liang, J., Ji, Y., Jiang, J.H., Yung, Y.L., Zhang, R., 2018. Radiative absorption enhancement of dust mixed with anthropogenic pollution over East Asia. Atmos. Chem. Phys. 18, 7815–7825.
Tindale, N., Pease, P., 1999. Aerosols over the Arabian Sea: atmospheric transport pathways and concentrations of dust and sea salt. Deep-Sea Res. II Top. Stud. Oceanogr. 46, 1577–1595.
Tobo, Y., Adachi, K., DeMott, P.J., Hill, T.C., Hamilton, D.S., Mahowald, N.M., Nagatsuka, N., Ohata, S., Uetake, J., Kondo, Y., 2019. Glacially sourced dust as a potentially significant source of ice nucleating particles. Nat. Geosci. 12, 253–258.
Trochkine, D., Iwasaka, Y., Matsuki, A., Yamada, M., Kim, Y.S., Nagatani, T., Zhang, D., Shi, G.Y., Shen, Z., 2003. Mineral aerosol particles collected in Dunhuang, China, and their comparison with chemically modified particles collected over Japan. J. Geophys. Res.-Atmos. 108.
Tuccella, P., Curci, G., Pitari, G., Lee, S., Jo, D.S., 2020. Direct radiative effect of absorbing aerosols: sensitivity to mixing state, brown carbon, and soil dust refractive index and shape. J. Geophys. Res.-Atmos. 125 e2019JD030967.
Tyrlis, E., Lelieveld, J., Steil, B., 2012. The summer circulation over the eastern Mediterranean and the Middle East: influence of the South Asian monsoon. Clim. Dyn. 40, 1103–1123.
Tyrlis, E., Škerlak, B., Sprenger, M., Wernli, H., Zittis, G., Lelieveld, J., 2014. On the linkage between the Asian summer monsoon and tropopause fold activity over the eastern Mediterranean and the Middle East. J. Geophys. Res.-Atmos. 119, 3202–3221.
van der Does, M., Knippertz, P., Zschenderlein, P., Harrison, R.G., Stuut, J.-B.W., 2018. The mysterious long-range transport of giant mineral dust particles. Sci. Adv. 4 eaau2768.
Vinoj, V., Satheesh, S.K., 2003. Measurements of aerosol optical depth over Arabian Sea during summer monsoon season. Geophys. Res. Lett. 30.
Vinoj, V., Rasch, P.J., Wang, H.L., Yoon, J.H., Ma, P.L., Landu, K., Singh, B., 2014. Short-term modulation of Indian summer monsoon rainfall by West Asian dust. Nat. Geosci. 7, 308–313.
Vukovic, A., Vujadinovic, M., Pejanovic, G., Andric, J., Kumjian, M.R., Djurdjevic, V., Dacic, M., Prasad, A.K., El-Askary, H.M., Paris, B.C., Petkovic, S., Nickovic, S., Sprigg, W.A., 2014. Numerical simulation of "an American haboob". Atmos. Chem. Phys. 14, 3211–3230.
Wang, B., LinHo, 2002. Rainy season of the Asian-Pacific summer monsoon. J. Clim. 15, 386–398.
Wang, C., Jeong, G.R., Mahowald, N., 2009a. Particulate absorption of solar radiation: anthropogenic aerosols vs. dust. Atmos. Chem. Phys. 9, 3935–3945.
Wang, C., Kim, D., Ekman, A.M.L., Barth, M.C., Rasch, P.J., 2009b. Impact of anthropogenic aerosols on Indian summer monsoon. Geophys. Res. Lett. 36.
Wang, B., Biasutti, M., Byrne, M.P., Castro, C., Chang, C., Cook, K., Fu, R., Grimm, A.M., Ha, K., Hendon, H., Kitoh, A., Krishnan, R., Lee, J., Li, J., Liu, J., Moise, A., Pascale, S., Roxy, M.K., Seth, A., Sui, C.H., Turner, A., Yang, S., Yun, K.S., Zhang, L., Zhou, T., 2021. **Monsoons Climate Change Assessment**. Bulletin of the American Meteorological Society 102, E1–E19.
Wang, B., Ding, Q., Liu, J., 2011. Concept of global monsoon. In: The Global Monsoon System: Research and Forecast. World Scientific, pp. 3–14.
Wang, P.X., Wang, B., Cheng, H., Fasullo, J., Guo, Z.T., Kiefer, T., Liu, Z.Y., 2014. The global monsoon across timescales: coherent variability of regional monsoons. Clim. Past 10, 2007–2052.
Wang, P.X., Wang, B., Cheng, H., Fasullo, J., Guo, Z., Kiefer, T., Liu, Z., 2017. The global monsoon across time scales: mechanisms and outstanding issues. Earth Sci. Rev. 174, 84–121.
Wang, X., Shi, T., Zhang, X., Chen, Y., 2020. An overview of snow albedo sensitivity to black carbon contamination and snow grain properties based on experimental datasets across the northern hemisphere. Curr. Pollut. Rep. 1–12.
Warren, S.G., Wiscombe, W.J., 1980. A model for the spectral albedo of snow. II: Snow containing atmospheric aerosols. J. Atmos. Sci. 37, 2734–2745.
Webb, N.P., Pierre, C., 2018. Quantifying anthropogenic dust emissions. Earth’s Future 6, 286–295.
Webster, P.J., 1987. The elementary monsoon. In: Monsoons. John Wiley and Sons, pp. 3–32.
Wonsick, M.M., Pinker, R.T., Ma, Y., 2014. Investigation of the "elevated heat pump" hypothesis of the Asian monsoon using satellite observations. Atmos. Chem. Phys. 14, 8749–8761.
Wu, G.X., Liu, Y.M., He, B., Bao, Q., Duan, A.M., Jin, F.F., 2012. Thermal controls on the Asian Summer Monsoon. Sci. Rep. 2.
Wu, G., He, B., Duan, A., Liu, Y., Yu, W., 2017. Formation and variation of the atmospheric heat source over the Tibetan Plateau and its climate effects. Adv. Atmos. Sci. 34, 1169–1184.
Xavier, P.K., Marzin, C., Goswami, B.N., 2007. An objective definition of the Indian summer monsoon season and a new perspective on the ENSO–monsoon relationship. Q. J. R. Meteorol. Soc. 133, 749–764.
Xi, X., Sokolik, I.N., 2015. Seasonal dynamics of threshold friction velocity and dust emission in Central Asia. J. Geophys. Res. Atmos. 120, 1536–1564.
Xu, C., Ma, Y., Yang, K., You, C., 2018. Tibetan plateau impacts on global dust transport in the upper troposphere. J. Clim. 31, 4745–4756.
Yasunari, T.J., Koster, R.D., Lau, W.K.M., Kim, K.M., 2015. Impact of snow darkening via dust, black carbon, and organic carbon on boreal spring climate in the Earth system. J. Geophys. Res.-Atmos. 120, 5485–5503.
Yu, P., Rosenlof, K.H., Liu, S., Telg, H., Thornberry, T.D., Rollins, A.W., Portmann, R.W., Bai, Z., Ray, E.A., Duan, Y., Pan, L.L., Toon, O.B., Bian, J., Gao, R.S., 2017. Efficient transport of tropospheric aerosol into the stratosphere via the Asian summer monsoon anticyclone. Proc. Natl. Acad. Sci. U. S. A. 114, 6972–6977.
Yuan, C., Lau, W.K.M., Li, Z., Cribb, M., 2019. Relationship between Asian monsoon strength and transport of surface aerosols to the Asian Tropopause Aerosol Layer (ATAL): interannual variability and decadal changes. Atmos. Chem. Phys. 19, 1901–1913.
Zender, C.S., 2003. Spatial heterogeneity in aeolian erodibility: Uniform, topographic, geomorphic, and hydrologic hypotheses. J. Geophys. Res. 108.
Zender, C.S., Miller, R., Tegen, I., 2004. Quantifying mineral dust mass budgets: terminology, constraints, and current estimates. EOS Trans. Am. Geophys. Union 85, 509–512.
Zhai, S., Jacob, D.J., Wang, X., Shen, L., Li, K., Zhang, Y., Gui, K., Zhao, T., Liao, H., 2019. Fine particulate matter (PM2.5) trends in China, 2013–2018: separating contributions from anthropogenic emissions and meteorology. Atmos. Chem. Phys. 19, 11031–11041.
Zhang, J., Reid, J.S., 2010. A decadal regional and global trend analysis of the aerosol optical depth using a data-assimilation grade over-water MODIS and Level 2 MISR aerosol products. Atmos. Chem. Phys. 10, 10949–10963.

Zhang, Q., Zheng, Y., Tong, D., Shao, M., Wang, S., Zhang, Y., Xu, X., Wang, J., He, H., Liu, W., Ding, Y., Lei, Y., Li, J., Wang, Z., Zhang, X., Wang, Y., Cheng, J., Liu, Y., Shi, Q., Yan, L., Geng, G., Hong, C., Li, M., Liu, F., Zheng, B., Cao, J., Ding, A., Gao, J., Fu, Q., Huo, J., Liu, B., Liu, Z., Yang, F., He, K., Hao, J., 2019a. Drivers of improved PM2.5 air quality in China from 2013 to 2017. Proc. Natl. Acad. Sci. U. S. A. 116, 24463–24469.

Zhang, T., Wang, T., Krinner, G., Wang, X., Gasser, T., Peng, S., Piao, S., Yao, T., 2019b. The weakening relationship between Eurasian spring snow cover and Indian summer monsoon rainfall. Sci. Adv. 5 eaau8932.

Zhao, B., Wang, Y., Gu, Y., Liou, K.-N., Jiang, J.H., Fan, J., Liu, X., Huang, L., Yung, Y.L., 2019. Ice nucleation by aerosols from anthropogenic pollution. Nat. Geosci. 12, 602–607.